Peer-reviewed version available at *Int. J. Mol. Sci.* **2019**, *20*, 579; doi:10.3390/ijms20030579

Catabolism of Fibromodulin in Developmental Rudiment and Pathologic Articular Cartilage demonstrate Novel Roles for MMP-13 and ADAMTS-4 in C-terminal Processing of SLRPs

Cindy Shu[1], Carl R Flannery[2], Christopher B Little[1, 3], James Melrose[1, 3, 4].

[1]Raymond Purves Research Laboratory, Institute of Bone & Joint Research, North Sydney Area Health Authority, Kolling Institute of Medical Research, University of Sydney, Royal North Shore Hospital, St. Leonards, NSW 2065, Australia.[2] Bioventus LLC, 4721 Emperor Blvd., Suite 100, Durham, NC 27703, USA.[3]Sydney Medical School, Northern, Royal North Shore Hospital. [4]Graduate School of Biomedical Engineering, University of New South Wales, Sydney, Australia

Corresponding author
James Melrose : james.melrose@sydney.edu.au

Raymond Purves Laboratory,
Level 10, Kolling Institute, B6,
Royal North Shore Hospital,
St. Leonards, New South Wales 2065,
Australia.

Tel No. +612 9926 4806 Fax No. +612 9926 5266

Key words: MMP-13, ADAMTS-4, FMOD, LUM, SLRPs, OA, PAMPs, DAMPs.

.

Abstract

Cartilage regeneration requires a balance of anabolic and catabolic processes. This study examined the susceptibility of fibromodulin (FMOD) and lumican (LUM) to degradation by MMP-13, ADAMTS-4 and ADAMTS-5, the three major degradative proteinases in articular cartilage in osteoarthritis (OA). Immunolocalisation of FMOD and LUM in foot sections of developmental cartilages demonstrated prominent localisations in metatarsal and phalangeal foetal rudiment cartilages and growth plate. An MMP-13 neoepitope antibody (TsYG11) demonstrated localisation of MMP-13 cleaved FMOD in the hypertrophic chondrocytes of the metatarsal growth plate. FMOD was more prominently localised in the superficial cartilage of normal and fibrillated zones in OA cartilage, TsYG11 positive FMOD was located deeper in the cartilage samples. Ab TsYG11 also identified FMOD fragmentation in Western blots of extracts of normal and fibrillated cartilage and total knee replacement OA cartilage. The C-terminal anti-FMOD used in this study (PR-184) failed to identify FMOD fragmentation due to C terminal processing, an equivalent Ab to the C-terminus of LUM (pAb PR-353) identified 3 prominent LUM fragments in OA human knee cartilages. In-vitro digestion of human knee cartilage with MMP-13, ADAMTS-4 and ADAMTS-5 generated equivalently sized FMOD fragments of 54, 45 and 32kDa to those in blots of OA cartilage, LUM was not less susceptible to fragmention in in-vitro digestions however Ab PR-353 detected N-terminally processed LUM fragments of 39, 38 and 22 kDa in 65-80 year old OA knee cartilage. FMOD and LUM were differentially processed during in-vitro digestions with MMP-13, ADAMTS-4 and ADAMTS-5 with FMOD susceptible to degradation by MMP-13, ADAMTS-4 and to a lesser extent ADAMTS-5 however LUM was less susceptible to fragmentation. FMOD was processed by MMP-13 in metatarsal and phalangeal foetal rudiment developmental cartilages and growth plate indicating a role in skeletogenesis.

Peer-reviewed version available at Int. J. Mol. Sci. 2019, 20, 579; doi:10.3390/ijms20030579

Introduction

The prevalence of knee OA has doubled since the mid 20th century despite the concerted efforts of the research and pharmaceutical industries over the last 5 decades to develop a therapeutic solution [1]. The global epidemic increase in BMI [2] may well have contributed to this higher incidence of OA [3, 4] through a combined effect of joint overloading and adiposity induced mild inflammation [5]. A Medline literature survey conducted in 2012 on OA and its associated medical costs based on 3 European, 6 North American and 2 Asian studies [6] showed that the annual cost of topical and oral NSAIDs for the treatment of OA was US$57.38 million. Hip and knee replacement costs exceeded US$1087.43 million and arthroscopic OA surgery US$1.71 million. Indirect lost economic productivity due to OA cost over US$ 4.1 billion, community services expenditure (US$ 5.25 million) and cost estimates for social services US$275 million [6]. A global OA study published in 2014 which examined the impact of knee and hip OA in 291 countries confirmed these major socioeconomic impacts [3]. Despite the pharmaceutical industry largely abandoning investigation into anti-arthritic biotherapeutics there remains a huge need to fully understand and treat OA in all of its complexities. Armed with a better understanding of key disease processes, the research and pharmaceutical communities will be in a better position to finally resolve the therapeutic alleviation of this apparently intractable disease.

The aim of the present study was to examine the susceptibility of fibromodulin (FMOD) and lumican (LUM) to degradation in cartilage development, maturation and pathology. FMOD and LUM are horse-shoe shaped class II members of the leucine rich repeat proteoglycan (SLRP) family [7]. FMOD and LUM are structurally homologous proteins

Peer-reviewed version available at Int. J. Mol. Sci. 2019, 20, 579; doi:10.3390/ijms20030579

sharing 47% identity in primary structure [8, 9]. Like all class II SLRPs FMOD and LUM contain 12 leucine rich repeat domains (LRRs) which provides them with interactive properties with a number of extracellular matrix (ECM) proteins. Foremost in these interactions which organise tissue form and function is the interaction of FMOD and LUM with type I and type II fibrillar collagens. FMOD and LUM interact with the same binding sites on type I collagen and regulate fibrillogenesis in-vitro[10]. FMOD-deficient mice have collagen fibrils of altered dimensions in tendons, and these mice display OA-like features in their knee articular cartilages [11, 12]. In addition, studies in knock-out mice indicate that LUM and FMOD reciprocally inhibit collagen interactions, through their binding sites on type I collagen [10]. The increased deposition of LUM in FMOD-deficient mice suggests that LUM binds to non-occupied FMOD-binding sites in collagen I [10]. FMOD and LUM are not redundant since they do not share functional equivalence in terms of how they organise ECM proteins in connective tissues. In the cornea lumican regulates the small regularly spaced orthogonal collagen fibre arrangements which are essential for optical clarity [13-19]. In contrast, fibromodulin is more prominent in the limbus and sclera where it stabilises large collagen fibre formation which provide mechanical stability to the eye-ball [15, 20, 21]. Results from FMOD knock-out mice also show that FMOD promotes formation of thick collagen fibres in tendon, whereas LUM forms thin collagen fibres [8].

FMOD has N-linked glycosylation sites at Asn 127, Asn 166, Asn 201, Asn 291, and Asn 341 of which 4 sites are occupied by keratan sulfate (KS) at any one time. LUM also contains four N-linked KS chains located within the central LRR region at Asn 88, Asn 127, Asn 160, and Asn 252. FMOD and LUM both contain clusters of N-terminal sulfated tyrosine residues, FMOD contains up to nine sulfated tyrosine residues and LUM two[22, 23]. These

are interactive with the heparin-binding proteins FGF-2, TSP-I, MMP-13, the NC4 domain of collagen IX, and IL-10. The tyrosine sulfate residues of FMOD also bind to collagen and promote fibril formation [24]. FMOD also sequesters TGF-β in the ECM and controls its bio-availability, binds C1q and activates the complement system[25-27]. LUM differs from FMOD in terms of its interactive properties with cells and the cellular responses it elicits. LUM impedes tumour growth, local invasion, intravasation and extravasation through its MMP-14 inhibitory activity, ability to affect focal adhesions and influence the migration properties and growth of tumour cells through its interactive properties with α2β1 integrin and its inhibitory effects on angiogenesis [28-30]. LUM also has novel roles in the innate immune response in the regulation of bacterial lipopolysaccharide sensing by Toll-like receptor-4 (TLR-4), in the presentation of bacterial lipopolysaccharide to CD14 and in the host response to this bacterial endotoxin [31]. LUM promotes bacterial phagocytosis [31, 32] and also regulates inflammation in connective tissues [33].

LUM and FMOD differ in their susceptibilities to degradation by metalloproteinases (MMPs). LUM was recently identified as an inhibitor of MMP-14 [34] and this is considered to contribute to its ability to regulate cell migration [35] and along with its interactive properties with α2β1 integrin to regulate angiogenesis and tumour growth [29]. LUM prevents cleavage of collagen by MMP-13 in-vitro or at least delays this reaction. In contrast to FMOD, LUM is not degraded by MMP-2, 3, 8, 9, 12, 13 [36]. In a study designed to examine the susceptibility of knee articular cartilage ECM components to MMP digestion, pieces of cartilage were used as substrates rather than soluble proteins and digestion was undertaken over 1-21 days. Evidence of proteolysis was determined by sequence identification of unique peptides generated by this procedure using a proteomics type

approach [36]. Peptides arising from types I, II, and III collagen, BGN, PRELP, FMOD, fibronectin, DCN, COMP, CILP, mimecan, aggrecan, and LUM were generated using MMP-2, 3, 8, 9, 12, 13, ADAMTS-4 and ADAMTS-5. ADAMTS-4 was the only MMP which degraded LUM releasing two small cleavage peptides, even so the abundance of these peptides was the least of any of the peptides generated in this study. Furthermore, LUM was resistant to degradation by all MMPs examined except MMP-12 which released 3 peptides. In comparison FMOD was extensively degraded by all MMPs tested with as many as 15 peptides generated by ADAMTS-4 and 18 peptides by MMP-12. The tyrosine sulfate rich region of FMOD is also cleaved by MMP-13. MMP-13 also cleaves the α1-IX collagen chain which resides on type II collagen fibrils in-situ (Danfelter et al 2007). This event precedes enzymatic attack of the type II collagen fibre.

In the present study we immunolocalised FMOD and its MMP-13 cleaved form in foetal human rudiment foot cartilage and in macroscopically normal and fibrillated human knee articular cartilage. In-vitro cleavage of FMOD and LUM by MMP-13 and ADAMTS-4 or -5 were also examined in macroscopically normal cartilage fragments and the cleavage peptides identified by Western blotting using antibodies to epitopes located in the N- and C-termini. The results obtained indicated that FMOD was degraded by MMP-13 in rudiment cartilage development, stimulated by treatment of knee articular cartilage with IL-1 and Oncostatin M in-vitro and was evident in pathological knee articular cartilage. In contrast, we found little evidence of cleavage of LUM by MMPs. The LUM fragmentation patterns we observed in aged human knee articular cartilage were therefore apparently due to another class of proteinase which awaits identification. BMP-1 is one proteinase of interest, BMP-1

processes mimecan/osteoglycin a related SLRP and enhances its ability to regulate collagen fibrillogenesis [37].

Results

We initially examined the immunolocalisation of FMOD and MMP-13 cleaved FMOD in the developmental phalangeal and metatarsal cartilage rudiments and metatarsal growth plate (Fig 1). This demonstrated the prominent distribution of full length FMOD in the foot rudiment cartilages associated with normal and hypertrophic chondrocytes (Fig 1a, d, g). MMP-13 cleaved FMOD displayed a similar distribution pattern in these tissues but was more prominently produced by the terminal hypertophic chondrocytes of the metatarsal growth plate (Fig 1h). This demonstrated that FMOD, and MMP-13 were associated with rudiment cartilage development and bone formation in the metatarsal growth plates.

Figure 1. Macroscopic vertical section through a 14 week gestational age human foetal foot stained with toluidine blue-fast green (macro) to depict the cartilage rudiments and the areas used for immunolocalisation(a-i). Immunolocalisation of FMOD (pAb PR-184) (a, d, g) and MMP-13 cleaved FMOD (pAb TsYG11)(b, e, h) in human foetal (14 weeks gestational age) metatarsal and phalangeal rudiment cartilage (a, b; d, e) and metatarsal growth plate (g, h). Negative control sections are also depicted for the same cartilage areas (c, f, i).

Preprints (www.preprints.org) | NOT PEER-REVIEWED | Posted: 24 December 2018 doi:10.20944/preprints201812.0274.v1

Peer-reviewed version available at *Int. J. Mol. Sci.* **2019**, *20*, 579; doi:10.3390/ijms20030579

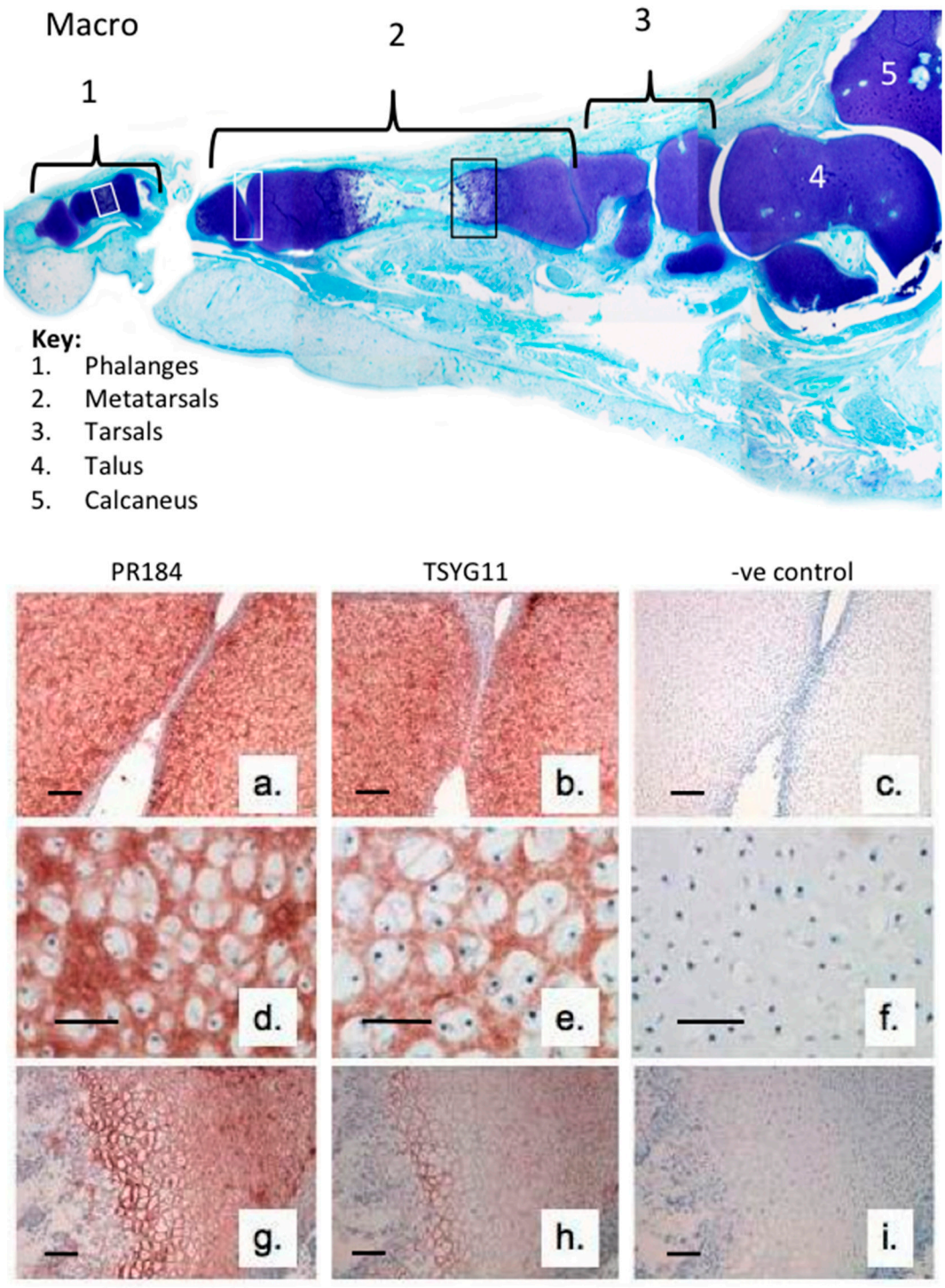

Figure 1. Macroscopic vertical section through a 14 week gestational age human foetal foot stained with toluidine blue-fast green (macro) to depict the cartilage rudiments and the areas used for immunolocalisation(a-i). Immunolocalisation of FMOD (pAb PR-184) (a, d, g) and MMP-13 cleaved FMOD (pAb TsYG11)(b, e, h) in human foetal (14 weeks gestational age) metatarsal and phalangeal rudiment cartilage (a, b; d, e) and metatarsal growth plate (g, h). Negative control sections are also depicted for the same cartilage areas (c, f, i).

Peer-reviewed version available at Int. J. Mol. Sci. 2019, 20, 579; doi:10.3390/ijms20030579

Visual macroscopic examination of human condyle articular cartilage identified areas of normal glistening macroscopically intact cartilage in the left knee of a 55 year old male donor (Fig 2a). The right knee of this donor however contained extensive areas of surface roughened and fibrillated cartilage (Fig2b). Four areas of degenerate cartilage were subsequently selected and one normal cartilage region in the left knee and these were extracted with 4M GuHCl. The constituent FMOD and LUM species in these tissue extracts were identified using Western blotting and specific C-terminal antibodies to FMOD (PR-184) and LUM (PR-353) in normal (Fig 2c) and in fibrillated cartilage (Fig2d,f). MMP-13 cleaved FMOD species were also identified on blots using pAb TsYG11 (Fig 2e). Very little fragmentation of FMOD was evident in the normal cartilage specimen (Fig 2c) or the finrillated cartilage zones using pAb PR-184 (Fig 2d). Multiple MMP-13 cleaved FMOD fragments were however evident in the 4 fibrillated cartilage zones examined (Fig 2d). Fragmentation of LUM was also evident in the normal and fibrillated cartilage zones using pAb-353 (Fig 2e). LUM fragmentation was particularly prominent in zone 3 (Fig 2e). Histological examination of proteoglycan distribution evident by toluidine blue-fast green staining in normal (Fig 2g) and fibrillated zone 4 (Fig 2j) cartilage regions in the lateral femoral condyles displayed distinct differences. The cartilage thickness was significantly less in the zone 4 specimen and proteoglycan levels severely depleted (compare Fig 2g with 2j). Immunolocalisation of FMOD and MMP-13 cleaved FMOD in the same cartilage regions demonstrated that full-length FMOD had a prominent distribution in the superficial cartilage and lower epitope levels deeper in the cartilages (Fig 2h, k) whereas MMP-13 cleaved FMOD was more prominently distributed in both the normal and fibrillated zone 4 (compare Fig 2i and 2l). In general FMOD was distributed around the cells presumably associated with collagenous networks in the interstitial matrix.

Preprints (www.preprints.org) | NOT PEER-REVIEWED | Posted: 24 December 2018 doi:10.20944/preprints201812.0274.v1

Peer-reviewed version available at Int. J. Mol. Sci. 2019, 20, 579; doi:10.3390/ijms20030579

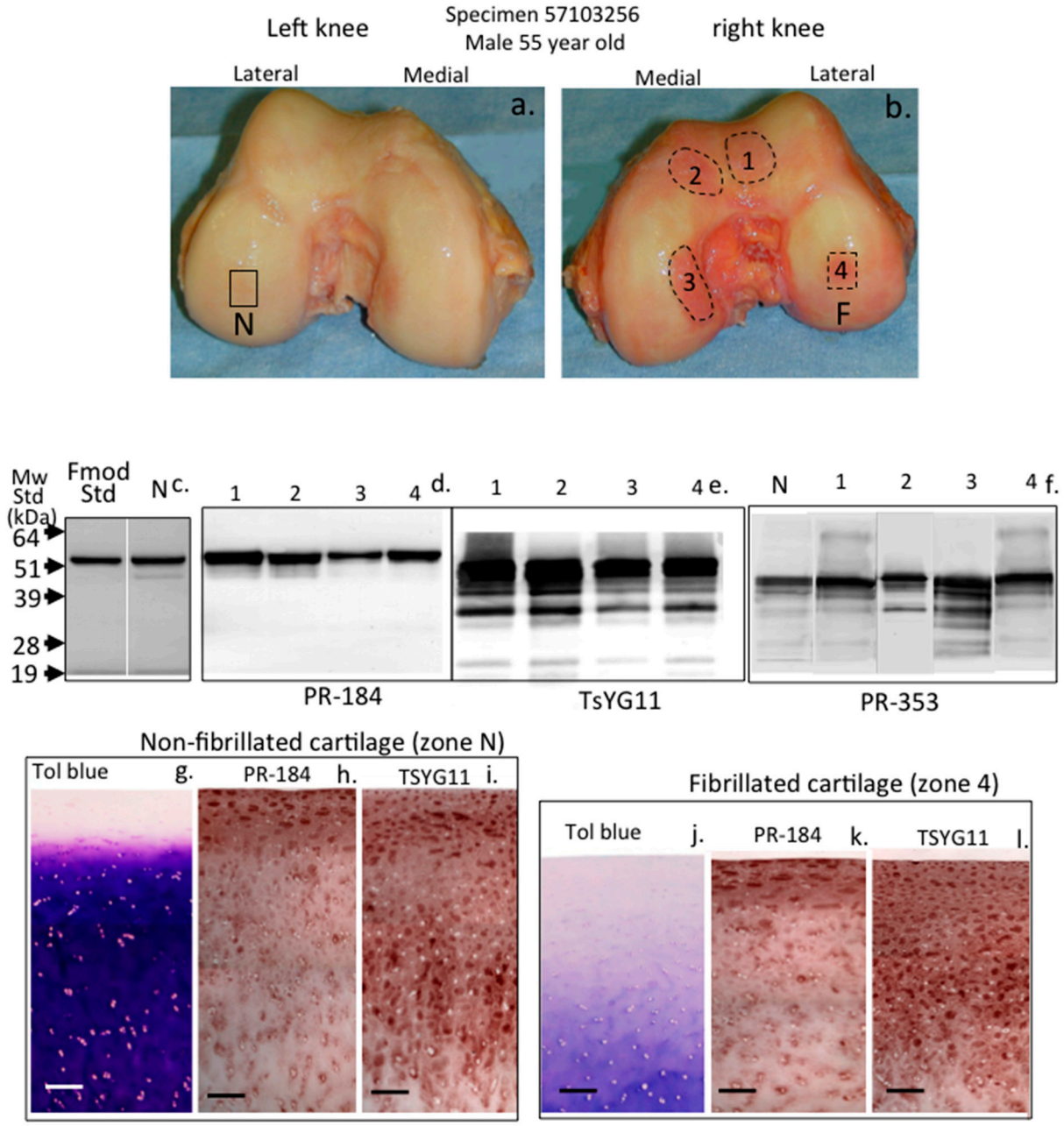

Figure 2. Macroscopic view of human knee femoral condyles from a 55 year old male (a, b) with a normal (N) area devoid of surface fibrillation and four areas of fibrillated cartilage (1-4) which were extracted with 4M GuHCl and analysed by Western blotting to identify FMOD (pAb PR-184) and MMP-13 cleaved FMOD (pAb TsYG11) and fragmented LUM (pAb PR-353) in these regions. Toluidine blue stained proteoglycan distributions in non-fibrillated (g) and fibrillated (j) and FMOD (h, k) and MMP-13 cleaved FMOD (i, l) were also immunolocalised in full thickness cartilage sections from the non-fibrillated region (N) and fibrillated zone 4 (F).

Figure 3 schematically depicts the amino acid sequences and locations of areas of the FMOD core protein identified by the PR-184 and TsYG11 antibodies (Fig 3a). MMP-13 fragmented

FMOD species were identified in extracts of normal non-degenerate and degenerate donor cartilages from total knee replacements aged 55, 58, 65, 73, 75 and 83 years of age (Fig 3b) Three prominent FMOD fragments were evident of 54, 45 and 32 kDa in size using the TsYG11 Ab (Fig 3b) however little if any fragmentation was detected using pAb PR-184 however the LUM band instensity was decreased in the older specimens (Fig 3c). Overnight enzymatic digestions of macroscopically normal articular cartilage from the femoral condyle of a 55 year old male donor using MMP-13, ADAMTS-4 and ADAMTS-5 also generated the three FMOD fragments of similar sizes to those present in Fig 3b (Fig 3d). These fragments were most prominent in the MMP-13 digests and were present in the tissue residue requiring release by GuHCl extraction as well as being detected in the digestion media. ADAMTS-4 and ADAMTS-5 also generated FMOD fragments of a similar size and detected using pAb TsYG11 to a lesser extent. Examination of the same digest sample blots with pAb PR-184 again failed to demonstrate FMOD fragmentation (Fig 3e). MMP-13 digests contained no detectable FMOD band indicating that this enzymatic treatment degraded the C-terminal epitope identified by pAb PR-184. The three main enzymatically generated FMOD fragments evident are presented schematically in Fig 3f.

Preprints (www.preprints.org) | NOT PEER-REVIEWED | Posted: 24 December 2018 doi:10.20944/preprints201812.0274.v1

Peer-reviewed version available at Int. J. Mol. Sci. 2019, 20, 579; doi:10.3390/ijms20030579

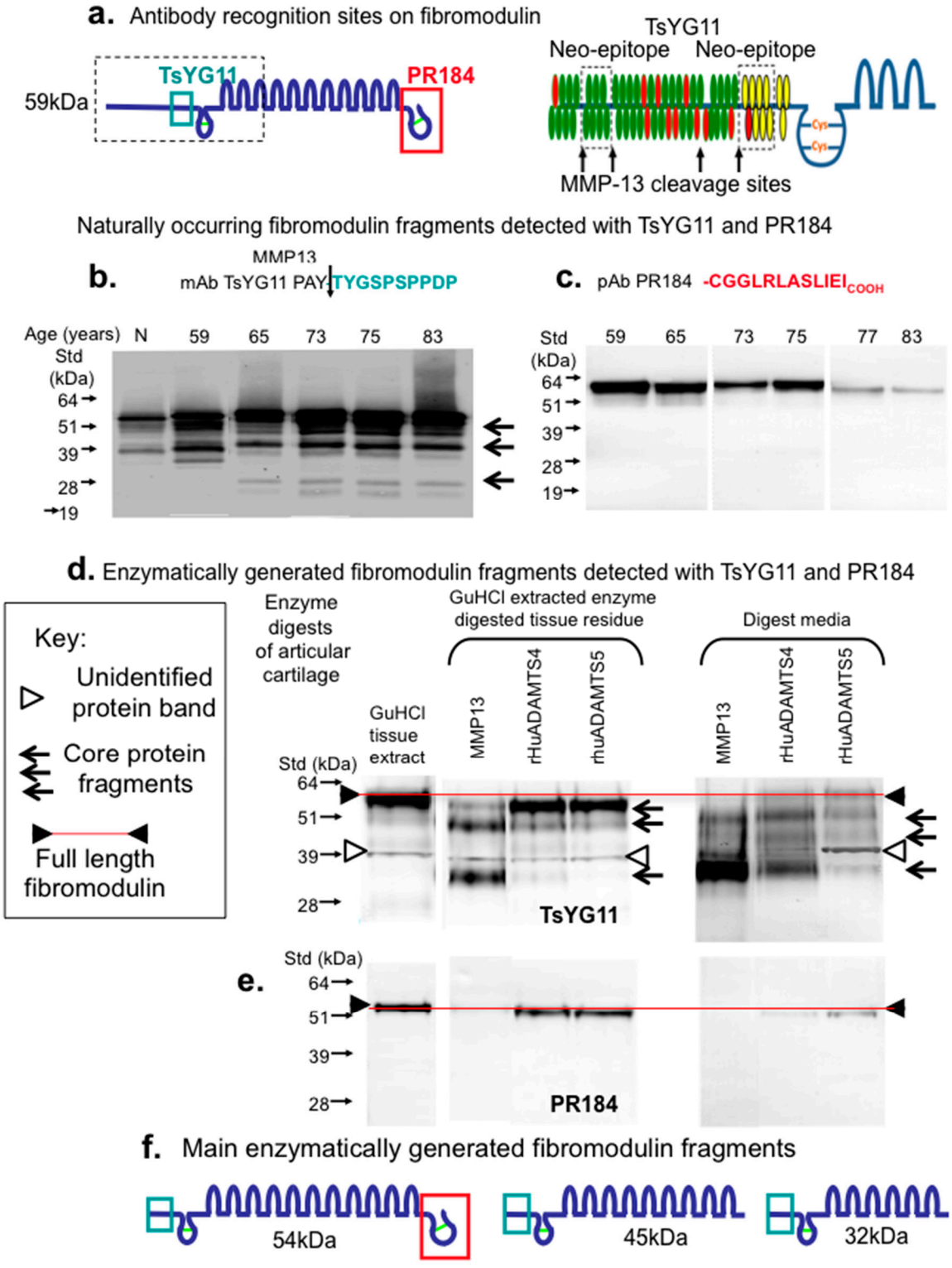

Figure 3. Schematic depiction of the epitopes identified by pAbs TsYG11 and PR-184 (a) and identification of naturally occurring FMOD fragments in OA knee cartilage from total knee replacement donors aged 59, 65, 75, 77 and 83 years of age using Western blotting and pAbs TsYG11 (b) and PR-184 (c) and FMOD species generated in-vitro by enzymatic digestion using MMP-13 , ADAMTS-4 and ADAMTS-5 detected using pAb TsYG11 (d) and pAb PR-184. Schematic depiction of the 3 major in-vitro generated FMOD fragments.

Examination of LUM fragmentation in knee cartilage extracts samples by immunoblotting demonstrated three prominent LUM fragments using pAb PR-353 (Fig 4a). These were most prominent in the 69-80 year old cartilage samples. Attempts to generate these LUM fragments by in-vitro digestion of cartilage samples with MMP-13, ADAMTS-4 or ADAMTS-5 failed to generate the same LUM fragmentation pattern (Fig 4b). While similar LUM fragments were detected in GuHCl control extracts of cartilage, these fragments were not evident in the MMP-13 digests suggesting that these may have been digested by MMP-13 however a full length LUM band was nevertheless also evident in the MMP-13 digests (Fig 4b). A LUM fragment was generated by ADAMTS-4 digestion slightly smaller than the 51kDa LUM and minor levels of the other 3 aforementioned LUM fragments. ADAMTS-5 did not generate appreciable levels of LUM fragments (Fig 4b). The LUM fragments observed are presented schematically in Fig 4c.

Preprints (www.preprints.org) | NOT PEER-REVIEWED | Posted: 24 December 2018 doi:10.20944/preprints201812.0274.v1

Peer-reviewed version available at Int. J. Mol. Sci. 2019, 20, 579; doi:10.3390/ijms20030579

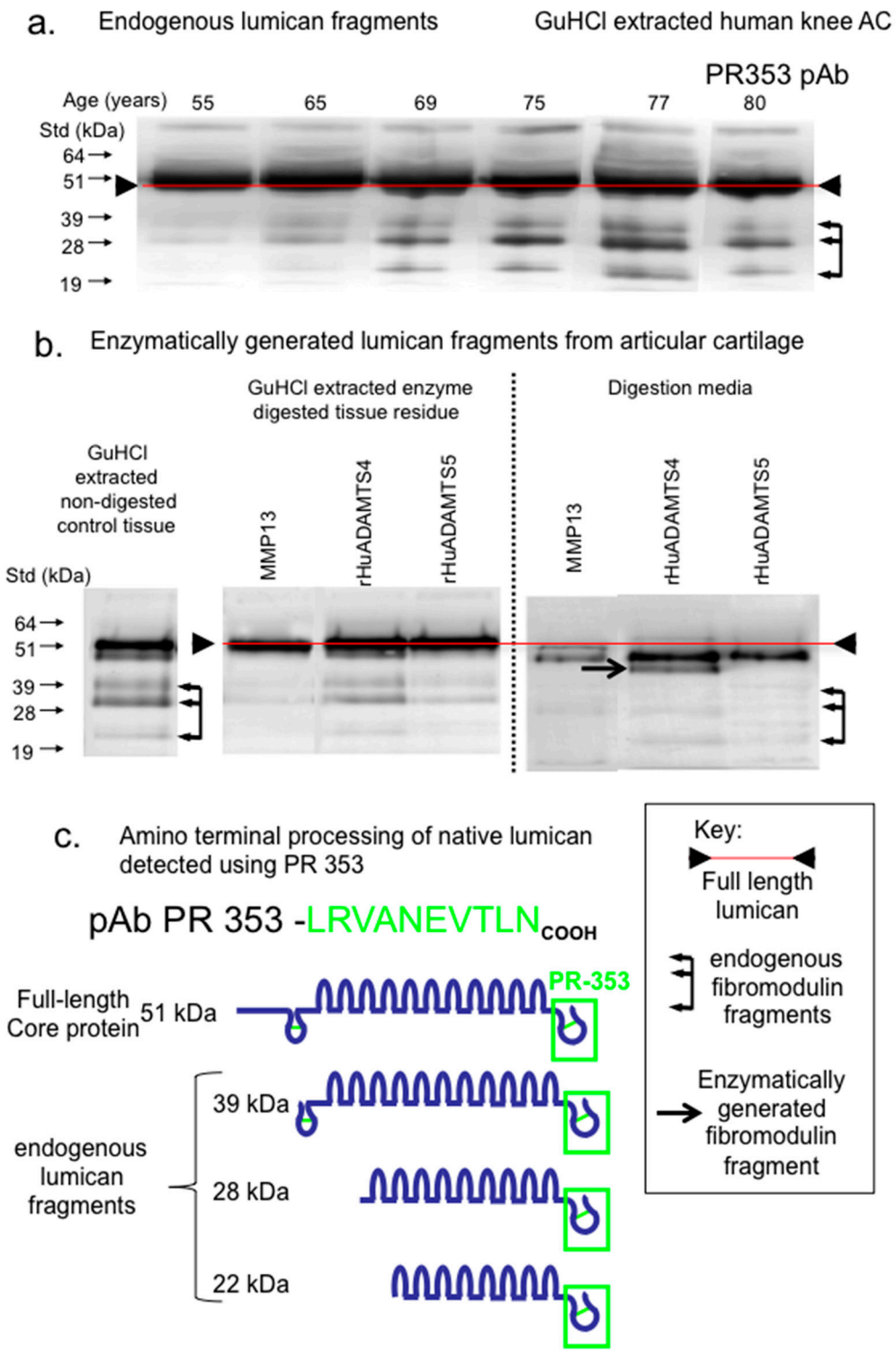

Figure 4. Composite figure depicting the naturally occurring LUM fragments in OA knee articular cartilage from total knee replacement donors aged 55, 65, 69, 75, 77 and 80 years of age (a) and released from macroscopically normal knee articular cartilage from the femoral condyle of a 55 year old donor by enzymatic digestion with MMP-13, ADAMTS-4 or ADAMTS-5 (b). Schematic depiction of the major naturally occurring LUM fragments in OA knee articular cartilage detected by pAb 353 on Western blots (c).

Examination of the autocatalytic conversion of ADAMTS-4 and ADAMTS-5 demonstrated the generated of a number of smaller molecular weight forms in ADAMTS-4 but to a lesser extent in the ADAMTS-5 preparation (Fig 5a). These samples were neverthess enzymatically active and aggrecanolysis of the aggrecan in the cartilage samples used displayed the typical BC-3 aggrecanase neoepitopes while MMP-13 or APMA did not (Fig 5b). MMP-13 (and APMA) did however generate the characteristic aggrecan MMP neoepitopes identified by MAb BC-14 (Fig 5b).

Preprints (www.preprints.org) | NOT PEER-REVIEWED | Posted: 24 December 2018 doi:10.20944/preprints201812.0274.v1

Peer-reviewed version available at Int. J. Mol. Sci. 2019, 20, 579; doi:10.3390/ijms20030579

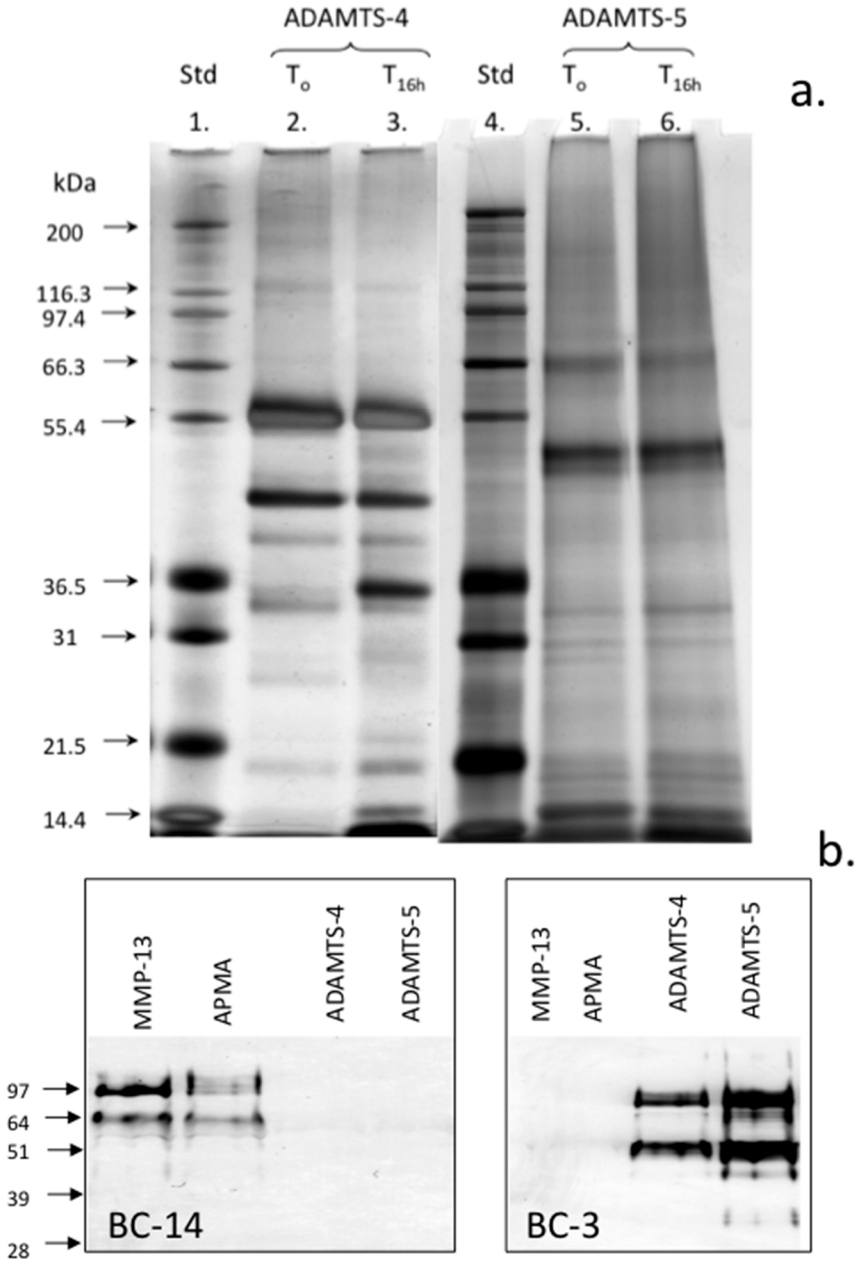

Figure 5. Assessment of autocatalytic conversion of ADAMTS-4 and 5 in-vitro. Silver stained LDS PAGE gel of the ADAMTS-4 and ADAMTS-5 species present following activation for 16h. Samples of ADAMTS-4, 5 were incubated at 37°C in MMP digestion buffer and aliquots removed after time zero and 16h incubation at 37°C and analysed in pre-poured Bis-Tris 10% NuPAGE gels (0.5 µg/lane) electrophoresed in MOPS running buffer. The gels were stained with a Novex Silver Stain kit to visualise ADAMTS species (a). Western blots demonstrating the generation of the BC-14 MMP neoepitope by MMP-13 digestion of human articular cartilage and generation of the BC-3 aggrecanase neoepitope in aggrecan by the activated ADAMTS-4 and 5 preparations (b). Broad range protein molecular weight standards (Novex) were used in lanes 1 and 4 for size calibrations and seeBlue 2 pre-stained standards for the Western blots.

Stimulation of cultured ovine explants with IL-1α and oncostatin-M resulted in a significant decline in sulfated glycosaminoglycan levels on day 5-12 of culture consistent with the stimulation of aggrecanolysis by this treatment (Fig 6a). Under the conditions used inclusion of an MMP inhibitor failed to prevent this decline in glycosaminoglycan levels. Cartilage collagen hydroxyproline values were largely unaffected by the IL-1α/oncostatin-M treatment (Fig 6b). Immunoblotting of media samples from the explant cultures demonstrated a reduction in FMOD levels on day 12 and the FMOD band was of a lower molecular weight than in control cultures (Fig 6c). Inclusion of PGE3162689 in the explant cultures prevented this shift in molecular weight to FMOD. At the concentration of PGE3162689 used MMP-1, -2, -3, -7, -8, -9, -13 and -14 were inhibited but not ADAMTSs in the cartilage explant cultures. While PGE3162689 prevented catabolism of FMOD it was incapable of preventing glycosaminoglycan loss from explant cultures stimulated with IL-1α and oncostatin-M indicating that this may be due to the action of ADAMTSs rather than MMPs.

Preprints (www.preprints.org) | NOT PEER-REVIEWED | Posted: 24 December 2018 doi:10.20944/preprints201812.0274.v1

Peer-reviewed version available at Int. J. Mol. Sci. 2019, 20, 579; doi:10.3390/ijms20030579

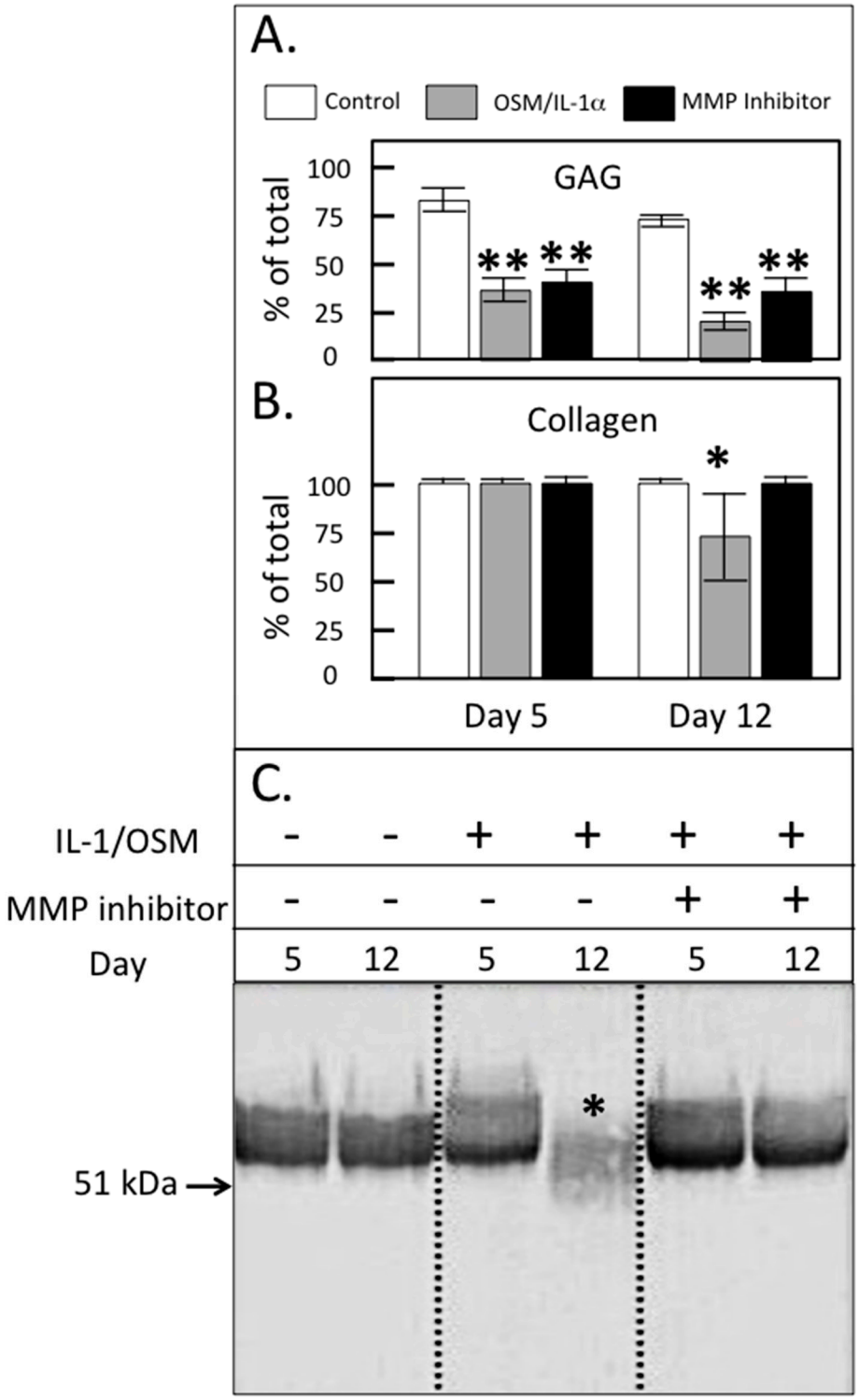

Figure 6. Glycosaminoglycan (GAG; A) and collagen content (B) of ovine articular cartilage explants after 5 or 12 days of culture in DMEM without (control) or with 5ng/ml IL-1 and 50ng/ml oncostatin M (IL-1/OSM) ± 300nm MMP-inhibitor (expressed as % of the total in explant plus media; mean ± standard deviation). Significant different between control and treated cultures * $p<0.05$, ** $p<0.01$. (C) Western blot analysis of FMOD core protein and fragments in the cartilage extracts using PR-184 recognising the C-terminus of FMOD.

Peer-reviewed version available at Int. J. Mol. Sci. 2019, 20, 579; doi:10.3390/ijms20030579

Discussion

SLRPs have important roles to play in the organisation of the cartilage ECM and functional roles in cartilage development, remodelling and in the pathogenesis of OA[42]. In the present study immunolocalisation of FMOD in the developmental metatarsal and phalangeal rudiment cartilages and metatarsal growth plate of the foot demonstrated FMOD was expressed by normal chondrocytes during cartilage development and by those chondrocytes undergoing hypertrophy in the growth plates. MMP-13 cleaved FMOD was prominent in the growth plates which is consistent with MMP-13 as a marker of hypertrophy and with roles for FMOD and MMP-13 in endochondral ossification. As shown in Figure 1, the foot has 28 bones and over 30 articulating joints and there are a number of small joints between these bones. These can all be affected by OA, this most commonly affects the hind-foot (sub-talar, talonavicular and calcaneocuboid), mid-foot (metatarsocunieform) and great toe (first metatarsophalangeal) joints.

OA is a progressive degenerative disorder affecting all joint tissues (articular cartilage, meniscus, synovium, subchondral bone, infrapatellar fat pad, ligaments) to variable degree [43, 44]. Historically, degeneration of articular cartilage has been a major focus of studies on the etiopathogenesis of OA. However, with the appreciation of OA as a multifactorial global disorder and that degenerative changes in cartilage are affected by degeneration in the synovium, subchondral bone, infra-patellar fat pad, meniscus, ligaments and tendons [43-53] there is now a greater appreciation of contributions from all these joint tissues in the achievement of optimal knee functional properties[54-57]. Results over the last few years have clearly shown that degenerative changes in the menisci, ligaments and tendons can exacerbate degenerative changes in the articular cartilage and may precede

these lesions [51-53]. The innate immune system and inflammation are also now recognized as key pathways in the onset and progression of OA through generation of a variety of damage associated molecular pattern molecules (DAMPs) which act through multiple pathways [58]. DAMPs reside inside the cell or are sequestered in the ECM thus are not normally identified by the innate immune system [59, 60]. In OA however, release of DAMPs from diseased/pathological tissues by proteases [61] makes them available to interact with pattern recognition receptors such as the Toll-like receptors (TLRs) and other non-immune cell-surface receptors which activate innate immune and inflammatory responses [62]. SLRPs can act as powerful DAMPs following their proteolytic release from the ECM, clustering different types of receptors to orchestrate a host of downstream signalling events [63-65].

Proteolytic activity by ADAMTS-4, ADAMTS-5 [66], MMP-2, MMP-3, MMP-13, MMP-14[36] during OA releases intact or fragmented forms of FMOD and LUM from articular cartilage and these act as DAMPs activating TLR2 and 4 initiating innate inflammation, and pain pathways [61, 65]. LUM also augments LPS signalling in the innate immune response through interaction with cell surface CD14 (monocyte differentiation factor) which is a co-receptor for bacterial lipopolysaccharide that also interacts with members of the TLR family leading to NFκB activation, cytokine secretion and the inflammatory response [65]. As shown by the findings of the present study, despite similarities in overall structure, FMOD and LUM display differential susceptibilities to degradation by MMPs and ADAMTS-4 and ADAMTS-5. FMOD is susceptible to degradation however LUM is resistant to MMP cleavage, this may be related to its recent identification as an MMP-inhibitor [34]. LUM binds to the catalytic domain of MMP-14 completely inactivating its activity in B16F1 melanoma cells [34]

Peer-reviewed version available at Int. J. Mol. Sci. 2019, 20, 579; doi:10.3390/ijms20030579

inhibiting the migration of melanoma cells and cell-matrix interactions required to promote tumor progression [30, 67]. This inhibitory activity resides in a peptide named lumcorin located in LRR-9 of LUM [68]. MT1-MMP however cleaves LUM abrogating the suppressive activity it displays towards tumor cell colony formation [69].

The tyrosine rich residues in the N terminal region of FMOD are sulfated [22], bind collagen enhancing fibril formation [24], and heparin binding bioactive factors [24] but are cleaved by MMP-13 [70]. FMOD in articular cartilage, intervertebral disc and meniscus is extensively fragmented in OA [71, 72] and in animal models of IVD and cartilage degeneration [39, 73]. FMOD also contains a number of small KS chains in its central LRR region [74, 75] which are interactive centres for a number of growth factors and morphogens [76]. In a proteomics microarray and plasmon resonance binding study corneal KS interacted with 217 of 8268 microarray proteins, including 75 kinases, several membrane and secreted proteins, cytoskeletal proteins, and many nerve function proteins. Of 85 ECM nerve-related epitopes in a secondary screen, KS bound 40 proteins, including Slit, 2 Robo's, 8 Ephrins, 8 semaphorins, and 2 nerve growth factor receptors [77]. The KS chains of FMOD can be capped by α(2-3)- , α(2-6)-linked N-acetylneuraminic acid or α(1-3) L-fucose residues which may modify their interactive properties [78]. Two pattern recognition C-type lectin DAMP receptors, SIGLEC (sialic acid binding Ig-like lectins) [79] and dendritic cell Langerin, identify sialylated KS and galactose-6 sulfate epitopes on KS[80-82]. Interaction of Langerin with a highly sulfated KS disaccharide has potent anti-inflammatory activity in emphysema and in a model of chronic obstructive pulmonary disease [80].

Peer-reviewed version available at *Int. J. Mol. Sci.* **2019**, *20*, 579; doi:10.3390/ijms20030579

In the present study, FMOD was present at a higher density in the superficial region than in the interterritorial matrix of mature knee articular cartilage [83]. MMP-13 cleaved FMOD was also prominent in the deep cartilage regions. FMOD fragmentation has been reported in RA and OA articular cartilage [84, 85] and with ageing [86]. We have recently reported minimal fragmentation of FMOD compared with other SLRPs in osteoarthritic knee menisci and knee and hip articular cartilage when a C-terminal antibody was used for FMOD detection [38]. Results of the present study indicate C-terminal processing of FMOD would have resulted in an inability to detect the processed forms of FMOD using Ab PR-184. Higher levels of FMOD mRNA have been observed in human OA cartilage and increased levels of translated protein indicative of an attempted repair response [84, 85]. FMOD enhances angiogenesis and has critical roles to play in cutaneous wound healing [87]. A deficiency of FMOD leads to delayed wound healing by detrimentally altering temporospatial expression of TGF-β ligands and receptors [87]. LUM also accelerates wound healing by enhancing α2β1 mediated fibroblast contractility at the wound site [88]. TNFα stimulated fibroblasts release elevated levels of LUM at wound sites promoting fibrocyte differentiation upregulating scar formation in healing wounds [89].

In cartilage degradation *in vitro*, FMOD is degraded in bovine nasal cartilage explant cultures stimulated with IL-1 [70, 90]. Cleavage in the N-terminal extension of FMOD resulted in release of all but one of its sulfated tyrosine residues [70]. In-vitro experiments demonstrated MMP-13 but not MMP-2,-3,-8, or -9, selectively cleaved at this N-terminal site but only when FMOD was bound to type II collagen and not when in free solution [70]. This work resulted in the development of a neoepitope antibody (TsYG11) to the MMP-13 generated cleavage sequence in bovine FMOD between residues 63 and 64 at $PAY^{63}\downarrow A^{64}YG$

Peer-reviewed version available at Int. J. Mol. Sci. 2019, 20, 579; doi:10.3390/ijms20030579

[70] which we used in the present study. Previous studies have demonstrated cleavage of soluble bovine FMOD by ADAMTS-4 and ADAMTS-5 [91, 92]. Enzymatic digestion of intact human cartilage also resulted in FMOD cleavage. In the present study we compared the pattern of naturally-occurring FMOD fragments in normal, fibrillated, and OA human cartilages using N- and C-termini FMOD Abs. Ab TsYG11 prominently immunolocalised FMOD fragments in the fibrillated cartilage samples whereas FMOD was prominently localised in the superficial cartilage by Ab PR-184. Ab PR-353 to an N-terminal LUM sequence detected fragmentation in the same tissue zones.

DAMPs [93] also known as danger-associated molecular patterns [94], can initiate and perpetuate a non-infectious inflammatory response alerting the body to tissue injury and contributing to wound healing [95]. Increased expression of DAMPs in OA [96] represent novel therapeutic targets [60]. Furthermore, DAMPs in OA detected by TLR-4 can result in the excitation of nociceptors providing a link between DAMPs and pain pathways [61]. DAMPs are highly variable depending on the cell type and injured tissue [65]. Protein DAMPs include heat-shock proteins, HMGB1 (high-mobility group box 1), and ECM protein fragments generated following tissue injury [97]. Non-protein DAMPs include ATP, uric acid, HS, HA fragments and DNA. A sophisticated series of pattern recognition proteins (PAMPs) have evolved to detect DAMPs in tissues. PAMPs include soluble and cell-bound lectins, the TLR family, cytosolic NOD-like (nucleotide-binding oligomerization domain-like) receptors [98]. Soluble lectin PAMPs include the collectin, ficolin, intelectin and pentraxin families, mannose binding lectin and surfactant proteins A and D. DC-SIGN (ICAM3-grabbing non integrin) produced by dendritic cells and macrophages, modulates adaptive immunity detecting high mannose, GlcNAc, Fuc, Lewis^x antigen and viral coat glycoprotein components

Peer-reviewed version available at Int. J. Mol. Sci. 2019, 20, 579; doi:10.3390/ijms20030579

of HIV-1, HCV, Dengue, CMV, Measles, Ebola and *Mycobacterium Tuberculosis*, *Mycobacterium leprae* and *Candida albicans* cell wall components. DC-SIGN co-ordinates with the TLRs to up-regulate NF B expression and an anti-inflammatory cytokine response [98]. TLRs recognise highly conserved structural motifs in DAMPs of microbial pathogens and dead or necrotic mammalian cells. DAMP-TLR interaction initiates expression of activator protein-1 (AP-1) and NF B and pro-inflammatory cytokines which direct the adaptive immune response alerting the body to danger, and promoting tissue regenerative processes[61, 65]. Inhibition of DAMP-mediated inflammatory responses is a promising strategy in the clinical management of OA [94, 95].

In the present study FMOD fragments in cartilage from total knee replacement tissue donors were compared to FMOD fragments generated by enzymatic digestion of age matched normal human articular cartilage using the three major degradative enzymes in OA cartilage (MMP-13, ADAMTS-4 and ADAMTS-5) and in an IL-1α/Oncostatin-M-stimulated explant model of progressive cartilage degradation. Ab TsYG11 identified FMOD fragments in specimens of advanced age similar to those seen in fibrillated cartilage from a 55 year old knee. Ab PR-184 did not demonstrate FMOD fragmentation although the intensity of the FMOD band identified in blots decreased with the onset of age possibly indicating a lower abundance of FMOD. Digestion of macroscopically intact articular cartilage with MMP-13 generated 3 FMOD fragments of Mw 54, 45 and 32kDa. ADAMTS-4 and 5 also generated FMOD fragments of 54 and 45 kDa. Examination of LUM fragmentation in ADAMTS-4 and ADAMTS-5 digested cartilage samples identified two prominent LUM fragments of 48 and 45kDa however in general LUM appeared resistant to proteolysis by MMPs. The enzymatically generated LUM fragments were not of comparable size to naturally occurring

LUM fragments in total knee replacement patients aged 69-80 years of age. These findings are in agreement with an earlier study where cartilage pieces were digested with MMP-2, 3, 8, 9, 12, 13 and ADAMTS-4 and 5 [36] and consistent with identification of LUM as a MMP-14 inhibitor [34]. Zhen et al digested pieces of cartilage with MMP-2, 3, 8, 9, 12, 13, ADAMTS-4 and ADAMTS-5 for 1-21 days and proteolysis was determined by identification of unique peptides generated by proteomic sequencing [36]. Peptides arising from types I, II, and III collagen, BGN, PRELP, FMOD, fibronectin, DCN, COMP, CILP, mimecan, aggrecan, and LUM were identified. ADAMTS-4 was the only MMP which degraded LUM releasing two small cleavage peptides however their abundance was the least of any of the peptides generated in this study. LUM was resistant to degradation by all MMPs examined except MMP-12 which released 3 peptides, ADAMTS-4 released 2 peptides from LUM. In comparison FMOD was extensively degraded by all MMPs with as many as 15 peptides generated by ADAMTS-4 and 18 peptides by MMP-12. The tyrosine sulfate rich region of FMOD is also cleaved by MMP-13, this effect was not observed when a soluble substrate was used but was evident when cartilage pieces were digested. This indicated that the conformation of the FMOD was critical for MMP-13 cleavage with FMOD probably residing on a type I collagen fibre in this study to provide an appropriate orientation for proteolysis. MMP-13 also cleaves the α1-IX collagen chain which resides on type II collagen fibrils in-situ [99]. This event precedes enzymatic attack of the type II collagen fibre.

To date, a single site has been identified in bovine FMOD that is cleaved by MMP-13, ADAMTS-4 and ADAMTS-5, generating a catabolite approximately 5-10kDa smaller than the full-length protein [70, 91, 92]. Such a naturally-occurring fragment was also identified in OA human knee cartilage. These TsYG11-positive fragments most likely arise from proteolysis at

the known MMP-13/ADAMTS cleavage site as well as one of several as yet unidentified cleavage sites in the C-terminus and LRRs. In the present study MMP-13 and ADAMTS-4 generated a significant 37kDa fragment also observed in the OA tissue extracts. This fragment is likely generated by cleavage at the N-terminal site. ADAMTS-4 and 5 have previously been reported to cleave FMOD at the same Tyr-Ala bond as MMP-13, with ADAMTS-5 potentially being more active against FMOD in solution-phase digests [91, 100]. In contrast, our results demonstrated that ADAMTS-4 showed greater activity against FMOD in cartilage, despite ADAMTS-5 showing superior aggrecanolytic activity in-vitro.

Our data supports previous reports [41, 70] that cleavage of FMOD occurs after the major breakdown of aggrecan but before significant collagenolysis occurs in-vitro, suggesting that removal of FMOD from the collagen fibril may be a prerequisite for collagen proteolysis. It is interesting that despite the apparent activity of ADAMTS enzymes against FMOD, their increase in early cartilage degradation stimulated by IL-1 [41] or IL-1/OSM in our studies, is apparently not associated with breakdown of this SLRP. It is unclear why cytokine-stimulated ADAMTS activity did not result in more significant FMOD cleavage. It is possible that the concentration of ADAMTS enzymes generated by cytokine-stimulation of chondrocytes may be sub-optimal compared to the levels we used in our in-vitro digests. The living chondrocytes in the cytokine-stimulated culture model better mimics the true in-vivo situation but may secrete other factors in response to cytokine stimulation that abrogate the activity of ADAMTS on FMOD. Thus despite the potential for ADAMTS enzymes, and ADAMTS-4 in particular, to cleave FMOD in cartilage, MMP-13 plays a more significant role in this process, confirming earlier findings with bovine FMOD [70]. Identification of specific fragments of FMOD that are released from cartilage, may provide useful biomarkers to

Peer-reviewed version available at Int. J. Mol. Sci. 2019, 20, 579; doi:10.3390/ijms20030579

monitor progression of cartilage degradation from early stage aggrecan loss to later collagenolysis and identify therapeutic molecular targets. The differential susceptibility of FMOD and LUM to enzymatic degradation by MMPs observed in the present study was a surprising finding but in keeping with a recent study which demonstrated that LUM was an MMP-14 inhibitor [34]. MMPs are generally considered the physiological modulators of connective tissue composition both in tissue development and in pathological degradation. However LUM appears to be susceptible either to an MMP other than that examined in this or the cited studies or another class of proteinase. A related SLRP member mimecan/osteoglycan is degraded by BMP-1 which converts it to a form with better interactive properties in collagen fibrillogenesis. A similar proteinase may also be responsible for the LUM fragmentation observed in pathological knee cartilage samples observed in the present study.

Materials and Methods

Consumables

All electrophoresis consumables, pre-poured gels, running buffer concentrates, blotting membranes, pre-stained protein molecular weight standards were obtained from Invitrogen, Mount Vic, Australia. Blotting consumables, NBT/BCIP substrates, alkaline phosphatase labeled secondary antibodies, development buffers were obtained from Bio-rad Laboratories Pty Ltd, Gladesville, NSW 2111, Australia. Chondroitinase ABC (*Proteus vulgaris)*, keratanase-I (*Pseudomonas sp.)* and guanidine hydrochloride (GuHCl) were obtained from Sigma-Aldrich Australia, Castle Hill, NSW, Australia. N-glycanase (peptide-N-glycosidase F) from *E.coli* was obtained from Genzyme, N. Ryde, NSW, Australia. Recombinant human pro-MMP-13 was a generous gift from Professor Gillian Murphy, University of Cambridge, UK.

Peer-reviewed version available at Int. J. Mol. Sci. 2019, 20, 579; doi:10.3390/ijms20030579

Recombinant human ADAMTS-4 and ADAMTS-5 were kindly supplied by Dr Carl Flannery, Wyeth, Cambridge, Mass, USA. Menzel and Glaser SuperFrost ultraPlus, positively charged microscope sides were obtained from Fisher Scientific, Braunschweig, GmbH. NovaRED peroxidase substrate was obtained from Vector Laboratories (Burlingame, CA, USA). Biotinylated anti-rabbit IgG secondary antibody, avidin HRP conjugate and non-protein block were obtained from Dako, Botany, NSW, Australia. Foetal calf serum was obtained from Trace Biosciences Pty. Ltd., Castle Hill, NSW, Australia.

Tissues

This study was approved by the Human Research Ethics Committee of the Royal North Shore Hospital; all discarded tissues at the time of knee-joint replacement surgery were obtained with informed consent. Non-arthritic knees were obtained from The International Institute of Advancement in Medicine (IIAM), Jessup, PA, USA; a division of the Musculoskeletal Foundation. Cartilage from these normal joints was harvested from regions with a normal smooth glistening surface (N) and regions with a dull appearance indicative of surface fibrillation. Human foetal feet (12-14 week gestational age) were obtained at the time of termination of pregnancy with ethical permission. Sheep stifle joint control tissues were obtained from related projects in our laboratory.

Antibodies

Affinity purified rabbit polyclonal antibodies to the C-terminal peptide sequence LRLASLIEI of human FMOD (Ab PR-184) were used as described earlier [38, 39]. The anti-C terminal LUM antibody used in this study was an affinity purified rabbit polyclonal antibody raised against the peptide sequence H-CGGLRVANEVTLN-OH which comprises an amino terminal cysteine

residue used for conjugation to ovalbumin for antibody production, two spacer glycine residues, and the carboxyl terminal 10 amino acids of human, bovine and chick LUM. The anti-LUM antibodies were purified by affinity chromatography using the same immunization peptide as ligand. A rabbit polyclonal antibody (TsYG11) to the ten amino acid linear sequence TYGSPSPPDP C-terminal to the putative MMP-13 cleavage site in human FMOD was generated to examine FMOD core protein fragmentation. Monoclonal antibodies to neoepitope sequences generated by cleavage of aggrecan by ADAMTS (ARGS…; antibody BC-3) or MMPs (FFGV…; BC-14) were provided as hybridoma culture supernatant by Professor Bruce Caterson and Dr Clare Hughes (Cardiff University) and used to confirm the ADAMT-4, 5 were enzymatically active prior to digestion of cartilage.

Extraction of tissues

Tissues were cut into small pieces using scalpels and extracted with 10 volumes of 4M GuHCl 0.5M sodium acetate pH 5.8 containing 10mM EDTA, 20mM benzamidine and 50mM 6-aminohexanoic acid using end-over end mixing for 48h at 4°C. The tissue residues were separated from the extracts by centrifugation and discarded. Tissue extracts were dialysed against 3 changes of milliQ water and freeze dried.

Chondroitinase ABC, keratanase-I and N-glycanase digestion of tissue extracts

Freeze dried tissue extracts were re-dissolved (2mg dry wt/ml) overnight in 100mM Tris 0.03M acetate buffer pH 6.5 at 4°C with constant end-over-end mixing and aliquots (0.5ml) were digested with chondroitinase ABC (0.1 U) and keratanase-I (0.05 U) overnight at 37°C. Selected tissue extracts were also digested with N-glycanase (PNGase F, Glyko laboratories). Briefly, chondroitinase ABC and keratanase-I digested samples were dialysed and freeze

dried, then re-dissolved in 20mM sodium phosphate buffer pH 7.5 (100 µl), denaturation solution (2% SDS, 1M 2-mercaptoethanol, 5 µl) was then added and the samples were heated at 100°C for 5 minutes, NP-40 detergent (15% v/v, 5µl) was then added, and–N-glycanase (4 µl/20mU) and the samples were incubated at 37°C for 3h.

SDS PAGE and detection of SLRP fragments by Western blotting

Aliquots of the chondroitinase ABC, keratanase-I, II or N-glycanase digested samples, containing tissue extracts from an equivalent wet weight of tissue (0.8mg/lane) were mixed with 4 x LDS PAGE application buffer (35µl) and 10X reducing agent (15µl) and re-dispersed in a total volume of 100µl. The samples were then heated at 70°C for 30 min, cooled and 25 µl aliquots were electrophoresed under reducing conditions on 10% NuPAGE Bis-Tris gels at 200V constant voltage for 50 min using NuPAGE MOPS SDS running buffer. The gels were electroblotted to nitrocellulose membranes (0.22µm) using NuPAGE transfer buffer supplemented with 10% methanol at 30V constant voltage for 1h. SeeBlue-2 pre-stained protein molecular weight standards were also electrophoresed for molecular weight calibration and to assess the blotting transfer efficiency. The blots were initially blocked for 3h with 5% BSA in 50mM Tris-HCl 0.15M NaCl pH 7.2 (TBS) then incubated with either PR-184 (0.5 µg/ml) or TsYG 11 (1/1000 diln) diluted in 2% BSA in TBS overnight at room temp. After a brief rinse in TBS, goat anti rabbit IgG alkaline phosphatase conjugate diluted in TBS (1/5000 dilution) was added, and after a further 1h the blots were washed in TBS (3 x10 minutes) and NBT/BCIP substrates were added in alkaline phosphatase development buffer (0.1M Tris-HCl pH 9.5 containing 5mM $MgCl_2$) for detection of immune complexes and the blots rinsed in milliQ distilled water and dried. Western blots were repeated a minimum of three times and also conducted omitting primary antibody to check that no IgG species were

Peer-reviewed version available at Int. J. Mol. Sci. 2019, 20, 579; doi:10.3390/ijms20030579

present in the tissue extracts which cross-reacted with the conjugated secondary antibodies (false positives).

Cartilage digestion with MMP-13, ADAMTS-4 and ADAMTS-5.

Full-thickness articular cartilage (AC) was harvested from macroscopically normal regions of a femoral condyle of a 55 year old male cadaver (see Figure 2). The tissue was finely diced and 10mg wet weight samples were aliquoted into eppendorf tubes. One cartilage sample was extracted directly with 4M GuHCl buffered in 0.5M sodium acetate pH 5.8 containing 10mM EDTA, 20mM benzamidine and 50mM 6-aminohexanoic acid (0.5ml) with constant end-over-end mixing for 48h at 4°C. The extract was then recovered by centrifugation and the tissue residue discarded. In further tubes, diced AC was dispersed in: (i) a solution of 1mM APMA and MMP-13 (50µg/ml) in MMP digestion buffer (50mM Tris HCl 150mM NaCl 5mM $CaCl_2$ 1mM Zn Cl_2 0.01% Brij 35 pH 7.5 (0.2ml)); (ii) 1mM APMA in MMP digestion buffer; (iii) ADAMTS-4 or (iv) ADAMTS-5 (50 µg/ml) in the same MMP digestion buffer without APMA. After 24h incubation at 37°C, the tissue residues were spun down and the digestion buffer collected. The tissue residues were extracted with 4M GuHCl + proteinase inhibitors (0.5ml) for 48h at 4°C, the extract collected, and the tissue residues discarded. The 4M GuHCl extracts and digestion buffer samples were dialysed against milliQ distilled water then freeze dried. The samples were reconstituted in 50mM Tris-acetate buffer pH 6.5 (0.2ml) and the glycosaminoglycan (GAG) content of an aliquot was determined using the 1,9-dimethylmethylene blue metachromatic dye binding assay procedure. Chondroitinase ABC (0.01U/10µg GAG), keratanase-I (0.01 U/10 µg GAG) and keratanase-II (0.1mU/10µg GAG) were added to the samples and they were digested overnight at 37°C. 4X LDS PAGE application buffer (80µl) + 30µl reducing agent were then added to the digested

samples and they were heated on a block at 70°C for 10min. The samples were electrophoresed using pre-poured 10% Bis-Tris gels and transferred to nitrocellulose for analysis by Western blotting. Gel loading was 10µgGAG/lane for BC-3, 20µg GAG /lane for BC-14, and for FMOD the extract or digest supernatant from an equal wet weight of tissue (0.8mg)/lane. Samples were pre-digested with chondroitinase ABC, keratanase-I and II as indicated above.

Ovine cartilage explant cultures.

Full-depth articular cartilage explants were harvested from the trochlear groove of 6-12 month old ovine knee joints and cultured at 37°C, 5%(v/v) CO_2 for 48 hours in Dulbecco's Modified Eagles Medium (DMEM; Sigma, Castle Hill, NSW, Australia) buffered with sodium bicarbonate 3.7 g/L (Fronine, Riverstone, NSW, Australia) and containing 10% (v/v) Foetal Calf Serum (FCS; Trace Biosciences Pty. Ltd., Castle Hill, NSW, Australia), 2 mM L-glutamine (ICN Biochemicals Inc., Aurora, OH, USA), and 50 µg/mL Gentamicin (Pharmacia Pty. Ltd., Bentley, WA, Australia). Explants were washed (3 x 5 minutes) in serum free DMEM and cultured individually in serum free DMEM ± 5ng/ml IL-1α plus 50ng/ml oncostatin M (IL-1/OSM; PeproTech Rocky Hill, NJ 08553 , United States) ± 300nm PGE3162689 (synthesized at Procter and Gamble, USA). As previously described, PGE3162689 at this concentration inhibited MMP-1, -2, -3, -7, -8, -9, -13 and -14 but not ADAMTSs in cartilage explant cultures [40]. Explants were cultured for 5 or 12 days with media changed at 5 days—(n = 8/treatment/time-point). At harvest, explants (n = 6 / group) were digested with papain, and GAG and hydroxyproline content of the tissue digests and associated media were measured [40]. The remaining two randomly selected explants were pooled and extracted with 4M GuHCl and the chondroitinase and keratanase digested extracts were analysed by Western

Peer-reviewed version available at Int. J. Mol. Sci. 2019, 20, 579; doi:10.3390/ijms20030579

blotting with an antibody recognising the C-terminus of bovine FMOD (PR-184) [41] as described above.

Histological processing of specimens.

Human foetal feet were fixed in Histochoice for 18h. Full thickness slices (3mm thick) of adult femoral articular cartilage were fixed for 48h in 10% neutral buffered formalin. The tissues were then dehydrated in graded ethanol solutions and finally with xylene and embedded in paraffin. The foot blocks underwent surface decalcification in 10mM EDTA for 2h prior to sectioning. Four micron vertical microtome sections were prepared and attached to positively charged microscope slides.

Toluidine blue staining of cartilage specimens

Cartilage sections (4 µm) were stained for 10 min with 0.04% (w/v) toluidine blue in 0.1 M sodium acetate buffer, pH 4.0, to visualize the anionic glycosaminoglycans followed by a 2-min counterstain in 0.1% (w/v) fast green FCF.

Immunolocalisation of FMOD and MMP-13 cleaved FMOD in cartilage tissue sections.

Tissue sections were rehydrated through graded ethanol washes and pre-digested with chondroitinase ABC (0.1 U) for 1h then with 0.3% H_2O_2 for 10 min to inactivate endogenous peroxidase activity and blocked with DAKO non-protein block. Primary antibodies to FMOD (PR-184, 0.5 µg/ml) or MMP-13 cleaved FMOD (TsYG11, 1/1000 dilution) in TBS containing 2% BSA were added to the sections and they were incubated overnight at 4°C. The sections were then washed in TBS and biotinylated secondary antibody (mouse anti rabbit IgG, 5 µg/ml) was added for 3h at room temperature. Colour development was undertaken with

avidin HRP conjugate using NovaRED peroxidase substrate for 20min at room temperature and the slides were washed and mounted. Negative control sections were also run omitting primary Ab or by substituting an irrelevant species specific primary antibody for the authentic one. Both yielded negative results.

Conclusions

During cartilage development, remodelling and ageing, Fibromodulin and Lumican are both processed to variable degree. Fibromodulin was susceptible to fragmentation by MMP-13, ADAMTS-4 and ADAMTS-5, the three major proteinases active during the development of OA but also with roles during cartilage development and remodelling. MMP-13 and ADAMTS-4 had prominent roles in C-terminal Processing of fibromodulin. Lumican however was relatively resistant to proteolysis by MMP-13, ADAMTS-4 and ADAMTS-5 which was consistent with the MMP inhibitor activity recently identified in this protein. Lumican and fibromodulin have roles in the innate immune response and may modulate innate immune responses through pattern recognition receptors of relevance in cartilage homeostasis.

Acknowledgements

The following surgeons from The Dept of Orthopaedic and Traumatic Surgery, Royal North Shore Public and Private Hospitals, St. Leonards, NSW Australia are thanked for collecting the surgical specimens we used in this study, A. Ellis, M. Coolican, D. Parker, S. Ruff, D. Papadimitriou. Assoc Prof RC Appleyard, Macquarie University is thanked for providing the normal age matched human cartilage samples. Ms Eileen Cole Dept of Orthopaedic and Traumatic Surgery is thanked for obtaining informed consent from donor patients as part of the tissue procurement process. Ms Susan Smith, Raymond Purves Lab, Kolling Institute, Royal NorthShore Hospital undertook all immunolocalisation procedures. Prof Gillian Murphy, University of Nottingham, UK is thanked for the rhMMP-13 used in this study. Prof Dick Heinegard (deceased), University of Uppsala, Sweden provided the TsYG11 antibody used in this study. Prof Peter Roughley (deceased), McGill University, Canada kindly provided the PR-184 and PR-353 rabbit polyclonal antibodies we used. The BC-3 and BC-14 neoepitope antibody hybridoma conditioned medias were supplied by Prof Clare Hughes and Prof Bruce Caterson, University of Cardiff, UK. This study was funded by NHMRC Project Grant 352562.

Author Contributions

Investigation, methodology, data curation, formal analysis, writing-original draft preparation CS, JM . Formal analysis, writing-review and editing, CRF. Conceptualization, writing- review and editing CBL. Original draft preparation, review and editing, supervision, resources, funding acquisition, conceptualization JM.

Conflicts of Interest

The authors have no conflicts or financial disclosures to make.

References

1. Wallace, I. J.; Worthington, S.; Felson, D. T.; Jurmain, R. D.; Wren, K. T.; Maijanen, H.; Woods, R. J.; Lieberman, D. E., Knee osteoarthritis has doubled in prevalence since the mid-20th century. *Proc Natl Acad Sci U S A* **2017,** 114, (35), 9332-9336.
2. Wluka, A. E.; Lombard, C. B.; Cicuttini, F. M., Tackling obesity in knee osteoarthritis. *Nat Rev Rheumatol* **2013,** 9, (4), 225-35.
3. Cross, M.; Smith, E.; Hoy, D.; Nolte, S.; Ackerman, I.; Fransen, M.; Bridgett, L.; Williams, S.; Guillemin, F.; Hill, C. L.; Laslett, L. L.; Jones, G.; Cicuttini, F.; Osborne, R.; Vos, T.; Buchbinder, R.; Woolf, A.; March, L., The global burden of hip and knee osteoarthritis: estimates from the global burden of disease 2010 study. *Ann Rheum Dis* **2014,** 73, (7), 1323-30.
4. Felson, D. T.; Lawrence, R. C.; Dieppe, P. A.; Hirsch, R.; Helmick, C. G.; Jordan, J. M.; Kington, R. S.; Lane, N. E.; Nevitt, M. C.; Zhang, Y.; Sowers, M.; McAlindon, T.; Spector, T. D.; Poole, A. R.; Yanovski, S. Z.; Ateshian, G.; Sharma, L.; Buckwalter, J. A.; Brandt, K. D.; Fries, J. F., Osteoarthritis: new insights. Part 1: the disease and its risk factors. *Ann Intern Med* **2000,** 133, (8), 635-46.
5. Robinson, W. H.; Lepus, C. M.; Wang, Q.; Raghu, H.; Mao, R.; Lindstrom, T. M.; Sokolove, J., Low-grade inflammation as a key mediator of the pathogenesis of osteoarthritis. *Nat Rev Rheumatol* **2016,** 12, (10), 580-92.
6. Chen, A.; Gupte, C.; Akhtar, K.; Smith, P.; Cobb, J., The Global Economic Cost of Osteoarthritis: How the UK Compares. *Arthritis* **2012,** 2012, 698709.
7. Iozzo, R. V.; Schaefer, L., Proteoglycan form and function: A comprehensive nomenclature of proteoglycans. *Matrix Biol* **2015,** 42, 11-55.
8. Ezura, Y.; Chakravarti, S.; Oldberg, A.; Chervoneva, I.; Birk, D. E., Differential expression of lumican and fibromodulin regulate collagen fibrillogenesis in developing mouse tendons. *J Cell Biol* **2000,** 151, (4), 779-88.
9. Kalamajski, S.; Oldberg, A., Homologous sequence in lumican and fibromodulin leucine-rich repeat 5-7 competes for collagen binding. *J Biol Chem* **2009,** 284, (1), 534-9.
10. Svensson, L.; Narlid, I.; Oldberg, A., Fibromodulin and lumican bind to the same region on collagen type I fibrils. *FEBS Lett* **2000,** 470, (2), 178-82.
11. Gill, M. R.; Oldberg, A.; Reinholt, F. P., Fibromodulin-null murine knee joints display increased incidences of osteoarthritis and alterations in tissue biochemistry. *Osteoarthritis Cartilage* **2002,** 10, (10), 751-7.
12. Svensson, L.; Aszodi, A.; Reinholt, F. P.; Fassler, R.; Heinegard, D.; Oldberg, A., Fibromodulin-null mice have abnormal collagen fibrils, tissue organization, and altered lumican deposition in tendon. *J Biol Chem* **1999,** 274, (14), 9636-47.
13. Chakravarti, S., Functions of lumican and fibromodulin: lessons from knockout mice. *Glycoconj J* **2002,** 19, (4-5), 287-93.
14. Chakravarti, S.; Magnuson, T.; Lass, J. H.; Jepsen, K. J.; LaMantia, C.; Carroll, H., Lumican regulates collagen fibril assembly: skin fragility and corneal opacity in the absence of lumican. *J Cell Biol* **1998,** 141, (5), 1277-86.
15. Chen, S.; Oldberg, A.; Chakravarti, S.; Birk, D. E., Fibromodulin regulates collagen fibrillogenesis during peripheral corneal development. *Dev Dyn* **2010,** 239, (3), 844-54.
16. Chen, S.; Young, M. F.; Chakravarti, S.; Birk, D. E., Interclass small leucine-rich repeat proteoglycan interactions regulate collagen fibrillogenesis and corneal stromal assembly. *Matrix Biol* **2014,** 35, 103-11.
17. Dunlevy, J. R.; Beales, M. P.; Berryhill, B. L.; Cornuet, P. K.; Hassell, J. R., Expression of the keratan sulfate proteoglycans lumican, keratocan and osteoglycin/mimecan during chick corneal development. *Exp Eye Res* **2000,** 70, (3), 349-62.
18. Hassell, J. R.; Birk, D. E., The molecular basis of corneal transparency. *Exp Eye Res* **2010,** 91, (3), 326-35.
19. Kao, W. W.; Funderburgh, J. L.; Xia, Y.; Liu, C. Y.; Conrad, G. W., Focus on molecules: lumican. *Exp Eye Res* **2006,** 82, (1), 3-4.
20. Johnson, J. M.; Young, T. L.; Rada, J. A., Small leucine rich repeat proteoglycans (SLRPs) in the human sclera: identification of abundant levels of PRELP. *Mol Vis* **2006,** 12, 1057-66.

21. Keenan, T. D.; Clark, S. J.; Unwin, R. D.; Ridge, L. A.; Day, A. J.; Bishop, P. N., Mapping the differential distribution of proteoglycan core proteins in the adult human retina, choroid, and sclera. *Invest Ophthalmol Vis Sci* **2012,** 53, (12), 7528-38.
22. Onnerfjord, P.; Heathfield, T. F.; Heinegard, D., Identification of tyrosine sulfation in extracellular leucine-rich repeat proteins using mass spectrometry. *J Biol Chem* **2004,** 279, (1), 26-33.
23. Tillgren, V.; Onnerfjord, P.; Haglund, L.; Heinegard, D., The tyrosine sulfate-rich domains of the LRR proteins fibromodulin and osteoadherin bind motifs of basic clusters in a variety of heparin-binding proteins, including bioactive factors. *J Biol Chem* **2009,** 284, (42), 28543-53.
24. Tillgren, V.; Morgelin, M.; Onnerfjord, P.; Kalamajski, S.; Aspberg, A., The Tyrosine Sulfate Domain of Fibromodulin Binds Collagen and Enhances Fibril Formation. *J Biol Chem* **2016,** 291, (45), 23744-23755.
25. Hildebrand, A.; Romaris, M.; Rasmussen, L. M.; Heinegard, D.; Twardzik, D. R.; Border, W. A.; Ruoslahti, E., Interaction of the small interstitial proteoglycans biglycan, decorin and fibromodulin with transforming growth factor beta. *Biochem J* **1994,** 302 (Pt 2), 527-34.
26. Soo, C.; Hu, F. Y.; Zhang, X.; Wang, Y.; Beanes, S. R.; Lorenz, H. P.; Hedrick, M. H.; Mackool, R. J.; Plaas, A.; Kim, S. J.; Longaker, M. T.; Freymiller, E.; Ting, K., Differential expression of fibromodulin, a transforming growth factor-beta modulator, in fetal skin development and scarless repair. *Am J Pathol* **2000,** 157, (2), 423-33.
27. Sjoberg, A.; Onnerfjord, P.; Morgelin, M.; Heinegard, D.; Blom, A. M., The extracellular matrix and inflammation: fibromodulin activates the classical pathway of complement by directly binding C1q. *J Biol Chem* **2005,** 280, (37), 32301-8.
28. Brezillon, S.; Pietraszek, K.; Maquart, F. X.; Wegrowski, Y., Lumican effects in the control of tumour progression and their links with metalloproteinases and integrins. *FEBS J* **2013,** 280, (10), 2369-81.
29. Niewiarowska, J.; Brezillon, S.; Sacewicz-Hofman, I.; Bednarek, R.; Maquart, F. X.; Malinowski, M.; Wiktorska, M.; Wegrowski, Y.; Cierniewski, C. S., Lumican inhibits angiogenesis by interfering with alpha2beta1 receptor activity and downregulating MMP-14 expression. *Thromb Res* **2011,** 128, (5), 452-7.
30. Stasiak, M.; Boncela, J.; Perreau, C.; Karamanou, K.; Chatron-Colliet, A.; Proult, I.; Przygodzka, P.; Chakravarti, S.; Maquart, F. X.; Kowalska, M. A.; Wegrowski, Y.; Brezillon, S., Lumican Inhibits SNAIL-Induced Melanoma Cell Migration Specifically by Blocking MMP-14 Activity. *PLoS One* **2016,** 11, (3), e0150226.
31. Wu, F.; Vij, N.; Roberts, L.; Lopez-Briones, S.; Joyce, S.; Chakravarti, S., A novel role of the lumican core protein in bacterial lipopolysaccharide-induced innate immune response. *J Biol Chem* **2007,** 282, (36), 26409-17.
32. Shao, H.; Lee, S.; Gae-Scott, S.; Nakata, C.; Chen, S.; Hamad, A. R.; Chakravarti, S., Extracellular matrix lumican promotes bacterial phagocytosis, and Lum-/- mice show increased Pseudomonas aeruginosa lung infection severity. *J Biol Chem* **2012,** 287, (43), 35860-72.
33. Vij, N.; Roberts, L.; Joyce, S.; Chakravarti, S., Lumican regulates corneal inflammatory responses by modulating Fas-Fas ligand signaling. *Invest Ophthalmol Vis Sci* **2005,** 46, (1), 88-95.
34. Pietraszek, K.; Chatron-Colliet, A.; Brezillon, S.; Perreau, C.; Jakubiak-Augustyn, A.; Krotkiewski, H.; Maquart, F. X.; Wegrowski, Y., Lumican: a new inhibitor of matrix metalloproteinase-14 activity. *FEBS Lett* **2014,** 588, (23), 4319-24.
35. Malinowski, M.; Pietraszek, K.; Perreau, C.; Boguslawski, M.; Decot, V.; Stoltz, J. F.; Vallar, L.; Niewiarowska, J.; Cierniewski, C.; Maquart, F. X.; Wegrowski, Y.; Brezillon, S., Effect of lumican on the migration of human mesenchymal stem cells and endothelial progenitor cells: involvement of matrix metalloproteinase-14. *PLoS One* **2012,** 7, (12), e50709.
36. Zhen, E. Y.; Brittain, I. J.; Laska, D. A.; Mitchell, P. G.; Sumer, E. U.; Karsdal, M. A.; Duffin, K. L., Characterization of metalloprotease cleavage products of human articular cartilage. *Arthritis Rheum* **2008,** 58, (8), 2420-31.
37. Ge, G.; Seo, N. S.; Liang, X.; Hopkins, D. R.; Hook, M.; Greenspan, D. S., Bone morphogenetic protein-1/tolloid-related metalloproteinases process osteoglycin and enhance its ability to regulate collagen fibrillogenesis. *J Biol Chem* **2004,** 279, (40), 41626-33.
38. Melrose, J., Fuller ES, Roughley, PJ, Smith, MM, Kerr, B, Hughes , CE, Caterson, B, Little, CB. , Fragmentation of Decorin, Biglycan, Lumican and Keratocan is elevated in Degenerate Human Meniscus, Knee and Hip Articular Cartilages compared to Age-matched Macroscopically Normal and Control Tissues. *Arthritis Res Ther* **2008,** 10, (4), R79.

39. Melrose, J.; Smith, S. M.; Fuller, E. S.; Young, A. A.; Roughley, P. J.; Dart, A.; Little, C. B., Biglycan and fibromodulin fragmentation correlates with temporal and spatial annular remodelling in experimentally injured ovine intervertebral discs. *Eur Spine J* **2007,** 16, (12), 2193-205.
40. Little, C. B.; Hughes, C. E.; Curtis, C. L.; Janusz, M. J.; Bohne, R.; Wang-Weigand, S.; Taiwo, Y. O.; Mitchell, P. G.; Otterness, I. G.; Flannery, C. R.; Caterson, B., Matrix metalloproteinases are involved in C-terminal and interglobular domain processing of cartilage aggrecan in late stage cartilage degradation. *Matrix Biol* **2002,** 21, (3), 271-88.
41. Sztrolovics, R.; Alini, M.; Mort, J. S.; Roughley, P. J., Age-related changes in fibromodulin and lumican in human intervertebral discs. *Spine* **1999,** 24, (17), 1765-71.
42. Ni, G. X.; Li, Z.; Zhou, Y. Z., The role of small leucine-rich proteoglycans in osteoarthritis pathogenesis. *Osteoarthritis Cartilage* **2014,** 22, (7), 896-903.
43. Favero, M.; Belluzzi, E.; Trisolino, G.; Goldring, M. B.; Goldring, S. R.; Cigolotti, A.; Pozzuoli, A.; Ruggieri, P.; Ramonda, R.; Grigolo, B.; Punzi, L.; Olivotto, E., Inflammatory molecules produced by meniscus and synovium in early and end-stage osteoarthritis: a coculture study. *J Cell Physiol* **2018**.
44. Favero, M.; Ramonda, R.; Goldring, M. B.; Goldring, S. R.; Punzi, L., Early knee osteoarthritis. *RMD Open* **2015,** 1, (Suppl 1), e000062.
45. Belluzzi, E.; El Hadi, H.; Granzotto, M.; Rossato, M.; Ramonda, R.; Macchi, V.; De Caro, R.; Vettor, R.; Favero, M., Systemic and Local Adipose Tissue in Knee Osteoarthritis. *J Cell Physiol* **2017,** 232, (8), 1971-1978.
46. Chang, J.; Liao, Z.; Lu, M.; Meng, T.; Han, W.; Ding, C., Systemic and local adipose tissue in knee osteoarthritis. *Osteoarthritis Cartilage* **2018,** 26, (7), 864-871.
47. Favero, M.; El-Hadi, H.; Belluzzi, E.; Granzotto, M.; Porzionato, A.; Sarasin, G.; Rambaldo, A.; Iacobellis, C.; Cigolotti, A.; Fontanella, C. G.; Natali, A.; Ramonda, R.; Ruggieri, P.; De Caro, R.; Vettor, R.; Rossato, M.; Macchi, V., Infrapatellar fat pad features in osteoarthritis: a histopathological and molecular study. *Rheumatology (Oxford)* **2017,** 56, (10), 1784-1793.
48. Goldring, S. R., Alterations in periarticular bone and cross talk between subchondral bone and articular cartilage in osteoarthritis. *Ther Adv Musculoskelet Dis* **2012,** 4, (4), 249-58.
49. Richter, M.; Trzeciak, T.; Owecki, M.; Pucher, A.; Kaczmarczyk, J., The role of adipocytokines in the pathogenesis of knee joint osteoarthritis. *Int Orthop* **2015,** 39, (6), 1211-7.
50. Scanzello, C. R.; Goldring, S. R., The role of synovitis in osteoarthritis pathogenesis. *Bone* **2012,** 51, (2), 249-57.
51. Fuller, E.; Little, C. B.; Melrose, J., Interleukin-1alpha induces focal degradation of biglycan and tissue degeneration in an in-vitro ovine meniscal model. *Exp Mol Pathol* **2016,** 101, (2), 214-220.
52. Fuller, E. S.; Smith, M. M.; Little, C. B.; Melrose, J., Zonal differences in meniscus matrix turnover and cytokine response. *Osteoarthritis Cartilage* **2012,** 20, (1), 49-59.
53. Melrose, J.; Fuller, E. S.; Little, C. B., The biology of meniscal pathology in osteoarthritis and its contribution to joint disease: beyond simple mechanics. *Connect Tissue Res* **2017,** 58, (3-4), 282-294.
54. Madry, H.; Kon, E.; Condello, V.; Peretti, G. M.; Steinwachs, M.; Seil, R.; Berruto, M.; Engebretsen, L.; Filardo, G.; Angele, P., Early osteoarthritis of the knee. *Knee Surg Sports Traumatol Arthrosc* **2016,** 24, (6), 1753-62.
55. Malempati, C.; Jacobs, C. A.; Lattermann, C., The Early Osteoarthritic Knee: Implications for Cartilage Repair. *Clin Sports Med* **2017,** 36, (3), 587-596.
56. Matsubara, H.; Okazaki, K.; Takayama, Y.; Osaki, K.; Matsuo, Y.; Honda, H.; Iwamoto, Y., Detection of early cartilage deterioration associated with meniscal tear using T1rho mapping magnetic resonance imaging. *BMC Musculoskelet Disord* **2015,** 16, 22.
57. Williams, A.; Winalski, C. S.; Chu, C. R., Early articular cartilage MRI T2 changes after anterior cruciate ligament reconstruction correlate with later changes in T2 and cartilage thickness. *J Orthop Res* **2017,** 35, (3), 699-706.
58. Liu-Bryan, R., Synovium and the innate inflammatory network in osteoarthritis progression. *Curr Rheumatol Rep* **2013,** 15, (5), 323.
59. Merline, R.; Schaefer, R. M.; Schaefer, L., The matricellular functions of small leucine-rich proteoglycans (SLRPs). *J Cell Commun Signal* **2009,** 3, (3-4), 323-35.
60. Rosenberg, J. H.; Rai, V.; Dilisio, M. F.; Agrawal, D. K., Damage-associated molecular patterns in the pathogenesis of osteoarthritis: potentially novel therapeutic targets. *Mol Cell Biochem* **2017,** 434, (1-2), 171-179.

61. Miller, R. E.; Belmadani, A.; Ishihara, S.; Tran, P. B.; Ren, D.; Miller, R. J.; Malfait, A. M., Damage-associated molecular patterns generated in osteoarthritis directly excite murine nociceptive neurons through Toll-like receptor 4. *Arthritis Rheumatol* **2015,** 67, (11), 2933-43.
62. Ricard-Blum, S.; Ballut, L., Matricryptins derived from collagens and proteoglycans. *Front Biosci (Landmark Ed)* **2011,** 16, 674-97.
63. Moreth, K.; Iozzo, R. V.; Schaefer, L., Small leucine-rich proteoglycans orchestrate receptor crosstalk during inflammation. *Cell Cycle* **2012,** 11, (11), 2084-91.
64. Nastase, M. V.; Janicova, A.; Roedig, H.; Hsieh, L. T.; Wygrecka, M.; Schaefer, L., Small Leucine-Rich Proteoglycans in Renal Inflammation: Two Sides of the Coin. *J Histochem Cytochem* **2018,** 66, (4), 261-272.
65. Schaefer, L., Complexity of danger: the diverse nature of damage-associated molecular patterns. *J Biol Chem* **2014,** 289, (51), 35237-45.
66. Stanton, H.; Melrose, J.; Little, C. B.; Fosang, A. J., Proteoglycan degradation by the ADAMTS family of proteinases. *Biochim Biophys Acta* **2011,** 1812, (12), 1616-29.
67. Jeanne, A.; Untereiner, V.; Perreau, C.; Proult, I.; Gobinet, C.; Boulagnon-Rombi, C.; Terryn, C.; Martiny, L.; Brezillon, S.; Dedieu, S., Lumican delays melanoma growth in mice and drives tumor molecular assembly as well as response to matrix-targeted TAX2 therapeutic peptide. *Sci Rep* **2017,** 7, (1), 7700.
68. Pietraszek, K.; Brezillon, S.; Perreau, C.; Malicka-Blaszkiewicz, M.; Maquart, F. X.; Wegrowski, Y., Lumican - derived peptides inhibit melanoma cell growth and migration. *PLoS One* **2013,** 8, (10), e76232.
69. Li, Y.; Aoki, T.; Mori, Y.; Ahmad, M.; Miyamori, H.; Takino, T.; Sato, H., Cleavage of lumican by membrane-type matrix metalloproteinase-1 abrogates this proteoglycan-mediated suppression of tumor cell colony formation in soft agar. *Cancer Res* **2004,** 64, (19), 7058-64.
70. Heathfield, T. F.; Onnerfjord, P.; Dahlberg, L.; Heinegard, D., Cleavage of fibromodulin in cartilage explants involves removal of the N-terminal tyrosine sulfate-rich region by proteolysis at a site that is sensitive to matrix metalloproteinase-13. *J Biol Chem* **2004,** 279, (8), 6286-95.
71. Brown, S.; Melrose, J.; Caterson, B.; Roughley, P.; Eisenstein, S. M.; Roberts, S., A comparative evaluation of the small leucine-rich proteoglycans of pathological human intervertebral discs. *Eur Spine J* **2012,** 21 Suppl 2, S154-9.
72. Melrose, J.; Fuller, E. S.; Roughley, P. J.; Smith, M. M.; Kerr, B.; Hughes, C. E.; Caterson, B.; Little, C. B., Fragmentation of decorin, biglycan, lumican and keratocan is elevated in degenerate human meniscus, knee and hip articular cartilages compared with age-matched macroscopically normal and control tissues. *Arthritis Res Ther* **2008,** 10, (4), R79.
73. Young, A. A.; Smith, M. M.; Smith, S. M.; Cake, M. A.; Ghosh, P.; Read, R. A.; Melrose, J.; Sonnabend, D. H.; Roughley, P. J.; Little, C. B., Regional assessment of articular cartilage gene expression and small proteoglycan metabolism in an animal model of osteoarthritis. *Arthritis Res Ther* **2005,** 7, (4), R852-61.
74. Lauder, R. M.; Huckerby, T. N.; Nieduszynski, I. A., The structure of the keratan sulphate chains attached to fibromodulin isolated from articular cartilage. *Eur J Biochem* **1996,** 242, (2), 402-9.
75. Plaas, A. H.; Neame, P. J.; Nivens, C. M.; Reiss, L., Identification of the keratan sulfate attachment sites on bovine fibromodulin. *J Biol Chem* **1990,** 265, (33), 20634-40.
76. Weyers, A.; Yang, B.; Solakyildirim, K.; Yee, V.; Li, L.; Zhang, F.; Linhardt, R. J., Isolation of bovine corneal keratan sulfate and its growth factor and morphogen binding. *FEBS J* **2013,** 280, (10), 2285-93.
77. Conrad, A. H.; Zhang, Y.; Tasheva, E. S.; Conrad, G. W., Proteomic analysis of potential keratan sulfate, chondroitin sulfate A, and hyaluronic acid molecular interactions. *Invest Ophthalmol Vis Sci* **2010,** 51, (9), 4500-15.
78. Lauder, R. M.; Huckerby, T. N.; Nieduszynski, I. A., Lectin affinity chromatography of articular cartilage fibromodulin: Some molecules have keratan sulphate chains exclusively capped by alpha(2-3)-linked sialic acid. *Glycoconj J* **2011,** 28, (7), 453-61.
79. Gonzalez-Gil, A.; Porell, R. N.; Fernandes, S. M.; Wei, Y.; Yu, H.; Carroll, D. J.; McBride, R.; Paulson, J. C.; Tiemeyer, M.; Aoki, K.; Bochner, B. S.; Schnaar, R. L., Sialylated keratan sulfate proteoglycans are Siglec-8 ligands in human airways. *Glycobiology* **2018,** 28, (10), 786-801.
80. Kizuka, Y.; Mishra, S.; Yamaguchi, Y.; Taniguchi, N., Implication of C-type lectin receptor langerin and keratan sulfate disaccharide in emphysema. *Cell Immunol* **2018**.
81. Ota, F.; Hirayama, T.; Kizuka, Y.; Yamaguchi, Y.; Fujinawa, R.; Nagata, M.; Ismanto, H. S.; Lepenies, B.; Aretz, J.; Rademacher, C.; Seeberger, P. H.; Angata, T.; Kitazume, S.; Yoshida, K.; Betsuyaku, T.; Kida, K.;

Yamasaki, S.; Taniguchi, N., High affinity sugar ligands of C-type lectin receptor langerin. *Biochim Biophys Acta Gen Subj* **2018,** 1862, (7), 1592-1601.

82. Tateno, H.; Ohnishi, K.; Yabe, R.; Hayatsu, N.; Sato, T.; Takeya, M.; Narimatsu, H.; Hirabayashi, J., Dual specificity of Langerin to sulfated and mannosylated glycans via a single C-type carbohydrate recognition domain. *J Biol Chem* **2010,** 285, (9), 6390-400.
83. Hedlund, H.; Mengarelli-Widholm, S.; Heinegard, D.; Reinholt, F. P.; Svensson, O., Fibromodulin distribution and association with collagen. *Matrix Biol* **1994,** 14, (3), 227-32.
84. Cs-Szabo, G.; Melching, L. I.; Roughley, P. J.; Glant, T. T., Changes in messenger RNA and protein levels of proteoglycans and link protein in human osteoarthritic cartilage samples. *Arthritis Rheum* **1997,** 40, (6), 1037-45.
85. Cs-Szabo, G.; Roughley, P. J.; Plaas, A. H.; Glant, T. T., Large and small proteoglycans of osteoarthritic and rheumatoid articular cartilage. *Arthritis Rheum* **1995,** 38, (5), 660-8.
86. Roughley, P. J.; White, R. J.; Cs-Szabo, G.; Mort, J. S., Changes with age in the structure of fibromodulin in human articular cartilage. *Osteoarthritis Cartilage* **1996,** 4, (3), 153-61.
87. Zheng, Z.; Jian, J.; Velasco, O.; Hsu, C. Y.; Zhang, K.; Levin, A.; Murphy, M.; Zhang, X.; Ting, K.; Soo, C., Fibromodulin Enhances Angiogenesis during Cutaneous Wound Healing. *Plast Reconstr Surg Glob Open* **2014,** 2, (12), e275.
88. Liu, X. J.; Kong, F. Z.; Wang, Y. H.; Zheng, J. H.; Wan, W. D.; Deng, C. L.; Mao, G. Y.; Li, J.; Yang, X. M.; Zhang, Y. L.; Zhang, X. L.; Yang, S. L.; Zhang, Z. G., Lumican Accelerates Wound Healing by Enhancing alpha2beta1 Integrin-Mediated Fibroblast Contractility. *PLoS One* **2013,** 8, (6), e67124.
89. Pilling, D.; Vakil, V.; Cox, N.; Gomer, R. H., TNF-alpha-stimulated fibroblasts secrete lumican to promote fibrocyte differentiation. *Proc Natl Acad Sci U S A* **2015,** 112, (38), 11929-34.
90. Sztrolovics, R.; White, R. J.; Poole, A. R.; Mort, J. S.; Roughley, P. J., Resistance of small leucine-rich repeat proteoglycans to proteolytic degradation during interleukin-1-stimulated cartilage catabolism. *Biochem J* **1999,** 339 (Pt 3), 571-7.
91. Gendron, C.; Kashiwagi, M.; Lim, N. H.; Enghild, J. J.; Thogersen, I. B.; Hughes, C.; Caterson, B.; Nagase, H., Proteolytic activities of human ADAMTS-5: comparative studies with ADAMTS-4. *J Biol Chem* **2007,** 282, (25), 18294-306.
92. Kashiwagi, M.; Enghild, J. J.; Gendron, C.; Hughes, C.; Caterson, B.; Itoh, Y.; Nagase, H., Altered proteolytic activities of ADAMTS-4 expressed by C-terminal processing. *J Biol Chem* **2004,** 279, (11), 10109-19.
93. Matzinger, P., Tolerance, danger, and the extended family. *Annu Rev Immunol* **1994,** 12, 991-1045.
94. Venereau, E.; Ceriotti, C.; Bianchi, M. E., DAMPs from Cell Death to New Life. *Front Immunol* **2015,** 6, 422.
95. Wilgus, T. A., Alerting the body to tissue injury: The role of alarmins and DAMPs in cutaneous wound healing. *Curr Pathobiol Rep* **2018,** 6, (1), 55-60.
96. Rosenberg, J. H.; Rai, V.; Dilisio, M. F.; Sekundiak, T. D.; Agrawal, D. K., Increased expression of damage-associated molecular patterns (DAMPs) in osteoarthritis of human knee joint compared to hip joint. *Mol Cell Biochem* **2017,** 436, (1-2), 59-69.
97. Amin, A. R.; Islam, A. B., Genomic analysis and differential expression of HMG and S100A family in human arthritis: upregulated expression of chemokines, IL-8 and nitric oxide by HMGB1. *DNA Cell Biol* **2014,** 33, (8), 550-65.
98. Melrose, J., Glycan Binding Proteins Use Glycan Molecular Recognition Motifs to Regulate Endoplasmic Protein Folding, Transport, Lysosomal Targeting, and as Pattern Recognition Receptors in Pathogen Surveyance and Innate Immunity. . *Advances in Medicine* **2017,** 114, 110-168.
99. Danfelter, M.; Onnerfjord, P.; Heinegard, D., Fragmentation of proteins in cartilage treated with interleukin-1: specific cleavage of type IX collagen by matrix metalloproteinase 13 releases the NC4 domain. *J Biol Chem* **2007,** 282, (51), 36933-41.
100. Fushimi, K.; Troeberg, L.; Nakamura, H.; Lim, N. H.; Nagase, H., Functional differences of the catalytic and non-catalytic domains in human ADAMTS-4 and ADAMTS-5 in aggrecanolytic activity. *J Biol Chem* **2008,** 283, (11), 6706-16.